Doctoral Dissertation

Functional analysis of enzymes involved in thiol-based redox metabolism in *Euglena gracilis*

（ユーグレナにおけるチオールレドックス代謝に関する酵素の機能解析）

Shun Tamaki

Supervisor

Prof. Takahiro Ishikawa

The United Graduate School of Agricultural Sciences,

Tottori University

2015

Acknowledgements

I am extremely grateful to my major supervisor Prof. Takahiro Ishikawa, Faculty of Life and Environmental Science, Shimane University for his great guidance. I am also grateful to him for several helpful suggestions during my research.

I would like to express my sincere gratitude to my co-supervisors Prof. Yoshihiro Sawa, Faculty of Life and Environmental Science, Shimane University, and Prof. Fumio Watanabe, Faculty of Agriculture, Tottori University for their encouragement, support, and discussion. I also wish to express my grateful to late Prof. Emeritus Hitoshi Shibata, Faculty of Life and Environmental Science, Shimane University, Assistant Prof. Takanori Maruta, Faculty of Life and Environmental Science, Shimane University, and Assistant Prof. Hiroyuki Ashida, Faculty of Life and Environmental Science, Shimane University for their kind advice and encouragement.

I am greatly indebted to Prof. Shigeru Shigeoka, Faculty of Agriculture, Kinki University for his valuable suggestions and vital review of my scientific papers.

I am also grateful to former and current members of my laboratory for their help and cooperation.

Shun Tamaki

ABBREVIATIONS

1-CysPrx	**1-cycteine peroxiredoxin**
2-CysPrx	**2-cycteine peroxiredoxin**
ANOVA	**analysis of variance**
APX	**ascorbate peroxidase**
AsA	**ascorbate**
BLAST	**basic local alignment search tool**
CAT	**catalase**
CM	**Cramer-Myers**
Cumene-OOH	**cumene hydroperoxide**
DHA	**dehydroascorbate**
DHAR	**dehydroascorbate reductase**
dsRNA	**double-stranded RNA**
DTNB	**5,5'-dithiobis(2-nitrobenzoic acid)**
EDTA	**ethylenediaminetetraacetic acid**
EF1α	**elongation factor 1α**
FAD	**flavin adenine dinucleotide**
FTR	**ferredoxin-dependent thioredoxin reductase**
GC-MS	**gas chromatography-mass spectrometry**
GPX	**glutathione peroxidase**
GR	**glutathione reductase**
GSH	**(reduced) glutathione**
GSH1	**γ-glutamylcysteine synthetase, glutamate cysteine ligase**
GSH2	**glutathione synthetase**
GSSG	**oxidized glutathione**
H_2O_2	**hydrogen peroxide**
IPTG	**isopropyl-1-thio-β-D-galactopyranoside**
KD	**knockdown**

KH	**Koren–Hutner**
MDA	**monodehydroascorbate**
MDAR	**monodehydroascorbate reductase**
NADH	**nicotinamide adenine dinucleotide**
NADPH	**nicotinamide adenine dinucleotide phosphate**
NTR	**NADPH-dependent thioredoxin reductase**
PCR	**polymerase chain reaction**
Prx	**peroxiredoxin**
RNAi	**RNA interference**
RNA-Seq	**RNA sequencing**
ROS	**reactive oxygen species**
RT-PCR	**reverse transcription polymerase chain reaction**
SD	**standard deviation**
SDS	**sodium dodecyl sulfate**
SDS-PAGE	**sodium dodecyl sulfate-polyacrylamide gel electrophoresis**
Se-Cys	**selenocysteine**
SL	**spliced leader**
SOD	**superoxide dismutase**
tAPX	**thylakoid membrane-bound ascorbate peroxidase**
***t*-BOOH**	***ter*-butylhydroperoxide**
TMHMM	**transmembrane helices based on a hidden Marcov model**
Trx	**thioredoxin**
TryP	**tryparedoxin peroxidase**
TRYR	**trypanothione reductase**
TS_2	**oxidized trypanothione**
$T(SH)_2$	**(reduced) trypanothione**
TXN	**tryparedoxin**
TXNPx	**tryparedoxin peroxidase**

CONTENTS

CHAPTER I
Introduction 1

CHAPTER II
Identification and functional analysis of peroxiredoxin isoforms in *Euglena gracilis* 8

CHAPTER III
Biochemical and physiological analyses of NADPH-dependent thioredoxin reductase isozymes in *Euglena gracilis* 34

CHAPTER IV
Comparative and functional analyses of glutathione reductase and trypanothione reductase in *Euglena graclis* 55

REFERENCES 67

PUBLICATIONS 77

SUMMARY 78

CHAPTER I
Introduction

Reactive oxygen species (ROS), such as hydrogen peroxide (H_2O_2), superoxide, singlet oxygen, and hydroxyl radical, are continuously produced as byproducts of aerobic metabolisms including photosynthesis and respiratory. While ROS cause oxidative damage to proteins, DNA, and lipids, ROS also function as signaling molecules involved in regulating many biological processes, such as growth, development, cell cycle, and responses to biotic and abiotic stress, in various organisms. In order to maintain an appropriate concentration of ROS and regulate their action, cells have developed many enzymatic and non-enzymatic antioxidative systems in various cellular compartments (Mittler et al., 2004; Apel and Hirt, 2004; Shigeoka and Maruta, 2014).

Thiol-based ROS metabolism

Photosynthetic organisms have developed various non-enzymatic and enzymatic systems. Non-enzymatic antioxidants include the major cellular redox buffers ascorbate (AsA) and glutathione (GSH). AsA is oxidized by ROS to monodehydroascorbate and dehydroascorbate, and GSH to oxidized glutathione (GSSG). Reduced states of the antioxidants are maintained by AsA-GSH cycle consisting of monodehydroascorbate reductase (MDAR), dehydroascorbate reductase (DHAR), and glutathione reductase (GR). A high ratio of reduced to oxidized ascorbate and GSH is essential for ROS scavenging in cells (Ishikawa and Shigeoka, 2008).

Enzymatic ROS scavenging systems in plants include superoxide dismutase (SOD), catalase, ascorbate peroxidase (APX), peroxiredoxin (Prx), and glutathione peroxidase (GPX) (**Figure I-1**). SOD catalyzes the dismutating reaction of superoxide to H_2O_2 (Bowler et al., 1991). Catalase, APX, Prx, and GPX subsequently detoxify H_2O_2. APX and Prx use AsA and thioredoxin (Trx) as electron donors, respectively (Shigeoka et al., 1980; Wood et al., 2003). Although it is known that animal GPX use GSH as an electron donor, plant GPX-like enzymes use Trx as an electron donor for their peroxidase activity (Iqbal et al., 2006), thus these enzymes have been classified as a subclass of Prx family. These peroxidases are localized in almost every cellular

compartment, including the cytosol, chloroplasts, mitochondria, and peroxisomes. The simultaneous presence of all these enzymes creates a complex network of peroxidases, and adjusts ROS signals for metabolisms and environmental responses (Mittler et al., 2004; Shigeoka and Maruta, 2014).

Prxs constitute a family of thiol-based peroxidases with conserved functions in all kingdoms of life (Dietz, 2003). Based on structural and catalytic properties, Prxs are classified into four types; 1-CysPrx, 2-CysPrx, type II Prx, and PrxQ. In addition to the reduction of H_2O_2, Prx proteins also detoxify organic peroxides and peroxinitrite (Poole et al., 2004). During peroxide reduction, Prxs undergo oxidation which renders them inactive. As they lack redox cofactors, they depend upon external electron donors Trxs for their subsequent regeneration in the catalytic cycle (Rouhier and Jacquot, 2002). Furthermore, Prxs have been shown to function as not only peroxidase, but also chaperone, modulator of redox signaling, and circadian oscillator (Sevilla et al., 2015), supported the physiological significance of Prxs.

Trxs are low molecular weight (~12 kDa) disulfide oxidoreductases, which regulate numerous cellular processes such as stress responses, DNA synthesis, photosynthesis, and respiration by thiol–disulfide exchange reactions in conjunction with a large number of enzymes and related proteins (Arnér and Holmgren, 2000). In most cases, Trxs use NADPH as reducing power in a reaction catalyzed by NADPH-dependent Trx reductase (NTR). The two-component redox system formed by Trx and NTR is called a Trx system, which found in almost types of organisms from bacteria to plants and animals. NTRs are able to transfer reducing power from NADPH to FAD, and then reduce the disulfide at the active site Cys residues of oxidized Trx (Schürmann and Jacquot, 2000). Based on their structural and catalytic properties, NTRs are divided into two major subclasses: small type with a low molecular mass (~35 kDa), which found in organisms including prokaryotes, fungi, plants and algae, and large type with a high molecular mass (~55 kDa) in some eukaryotes including animals and protists (Jacquot et al., 2009). Photosynthetic organisms such as plants and algae possess the additional NTR enzyme, called NTRC, formed by an NTR domain at the N-terminus, and a Trx domain at the C-terminus (Serrato et al., 2004). The reverse genetic analyses using *Arabidopsis ntr* knockout mutants have demonstrated that NTRs play an essential role in various biological processes such as stress tolerances (Serrato

et al., 2004), development (Kirchsteiger et al., 2012), and metabolic processes including the biosynthesis of starch and chlorophyll (Michalska et al., 2009; Richter et al., 2013).

GSH is a low-molecular-weight thiol tripeptide, constituted by glutamate (Glu), cysteine (Cys), and glycine (Gly), in all organisms. As described above, GSH is an important component of AsA-GSH cycle, and also act on the direct scavenging of hydroxyl radical and singlet oxygen, protection of enzyme thiol groups, and signal transduction (Foyer and Noctor, 2005). For most of its functions, GSH must be in the reduced form. GR ensures that GSH remains at a reduced form and subsequently maintains a high GSH/GSSG ratio. GR belongs to the family of NADPH-dependent disulfide oxidoreductase as well as NTR, and is conserved in almost organisms. GR plays an essential role in ROS scavenging and various stress tolerance by efficiently maintaining the cellular reduced GSH pool (Gill et al., 2013).

In protozoan parasites trypanosomatids, however, most of their glutathione content is found in the form of a unique thiol, N^1,N^8-bis(glutathionyl)spermidine, also known as trypanothione ($T(SH)_2$). $T(SH)_2$ has been proved to play a central role in ROS metabolism, AsA homeostasis, DNA synthesis, and detoxification of metal drugs, as well as Trx and GSH in other organisms (Müller et al., 2003). These reactions require reduced form of $T(SH)_2$, and generate its oxidized form. For its function, $T(SH)_2$ is kept reduced by trypanothione reductase (TRYR). TRYR also belongs to the protein family of NADPH-dependent disulfide oxidoreductases. Thus, trypanosomatids possess a peculiar redox metabolism that is based on the $T(SH)_2$ and TRYR, but lack genes encoding GR and NTR.

ROS metabolism in trypanosomatids is mainly carried out by three distinct peroxidases: 2-CysPrx, GPX-like enzyme, and APX (Castro and Tomás, 2008) (**Figure I-1**). During the catalytic cycle, 2-CysPrx and GPX-like enzyme use tryparedoxin (TXN), thioredoxin-related protein with the atypical active site, as electron donor. The resulting oxidized TXN is reduced by $T(SH)_2$, but not NADPH-dependent oxidoreductase. APX also depends on $T(SH)_2$, in this case for regeneration of AsA from dehydroascorbate. Therefore, there are many ways to reduce ROS in trypanosomatids, but they entirely depend on $T(SH)_2$. The physiological importance of 2-CysPrxs in parasite survival and infection has been demonstrated by overexpression

and RNA interference approaches (Piñeyro et al., 2008; Wilkinson et al., 2003).

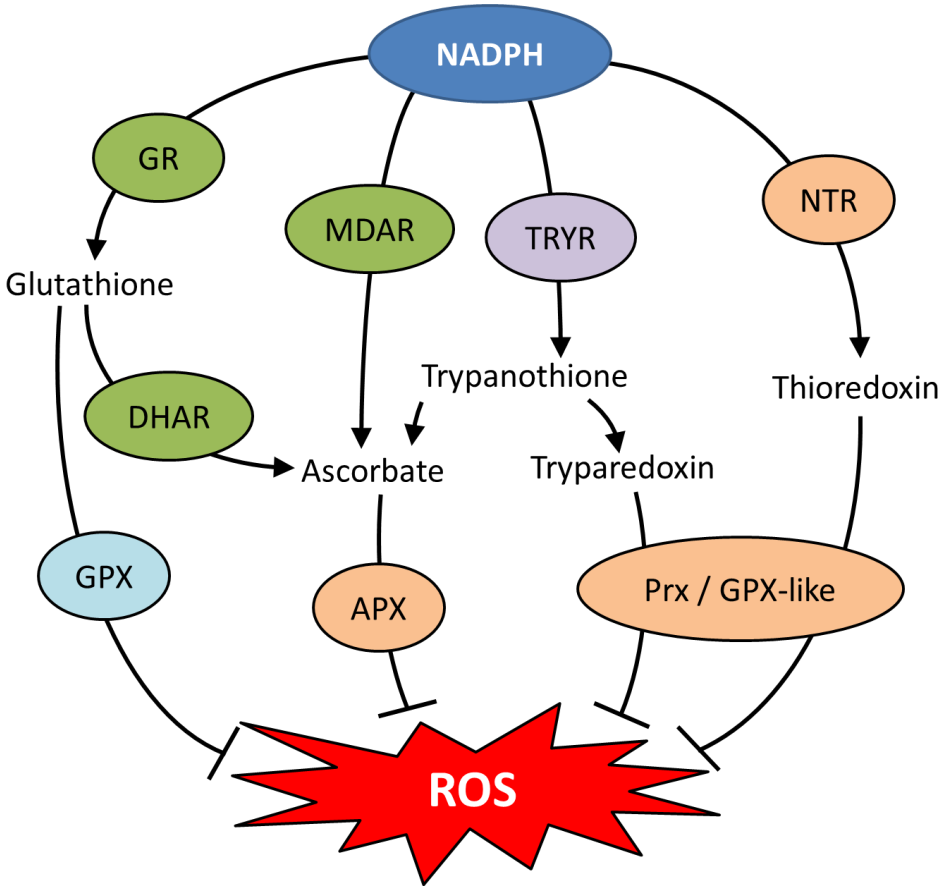

Figure I-1. Thio-based ROS metabolic pathways in plants and trypanosomatids. APX, ascorbate peroxidase; DHAR, dehydroascorbate reductase; GPX, glutathione peroxidase; GPX-like, thioredoxin or tryparedoxin-dependent GPX-like enzyme; GR, glutathione reductase; MDAR, monodehydroascorbate reductase; NTR, NADPH-dependent thioredoxin reductase; Prx, peroxiredoxin; TRYR, trypanothione reductase. Enzymes on a green background are found in plants, purple in trypanosomatids, orange in both plants and trypanosomatids, and blue is absent in both organisms.

ROS metabolism in Euglena

Euglena gracilis is a unicellular phytoflagellate, which belongs to the protist phylum Euglenozoa as well as trypanosomatids. *Euglena* shows characteristics of both plants and animals, and also possesses unique cell membrane complex, the pellicle complex, and metabolic pathway, including wax ester fermentation (Nakano et al., 1987; Inui et al., 1982). While ROS metabolism in other eukaryotic algae remains unclear, we have been studying APX-mediated ROS metabolism in *Euglena* (Rapolu et al., 2003; Ishikawa et al., 2010) (**Figure I-2**).

Euglena, which lacks catalase, contains a single APX, which is restricted to the cytosol with no isoform found in other organelles. This enzyme forms a unique intramolecular dimer, and can reduce both of H_2O_2 and alkyl hydroperoxides. In addition, silencing analysis using *Euglena* cells indicated physiological importance of APX in the metabolism of cellular H_2O_2 levels (Ishikawa et al., 2010). Activities of MDAR, DHAR, and GR, which constitute the AsA-GSH cycle, have been also located solely in the cytosol (Shigeoka et al., 1987a). Fructose-1,6-/sedoheptulose-1,7-bisphosphatase, $NADP^+$-glyceraldehyde-3-phosphate dehydrogenase, and ribulose-5-phosphate kinase enzymes of Calvin cycle in *Euglena* is not susceptible to H_2O_2 up to 1 mM, indicating the resistance of photosynthesis to H_2O_2 (Takeda et al., 1995). H_2O_2 formed in chloroplasts and mitochondria diffuses into the cytosol, where it is then decomposed by APX (Ishikawa et al., 1993). These findings may explain the physiological importance of cytosolic redox regulation in this alga. On the other hand, the existence of ROS metabolic enzyme in chloroplasts and mitochondria, which are major ROS source during aerobic metabolisms, remains unclear.

In contrast to plant GPX-like enzyme, *Euglena* contains GPX enzyme, which use GSH as electron donor (Overbaugh and Fall, 1985), while the gene encoding this enzyme has not yet been identified. Also, there is no biochemical and genetic information on Prx and Trx system constitutive enzymes in this alga. It have been demonstrated the existence of TRYR enzyme in *Euglena* (Montrichard et al., 1999), suggested the unique and complex thiol-based redox network in *Euglena*. Therefore, functional analysis of enzymes involved in thiol-based redox regulation will be required for understanding on entire ROS metabolism in *Euglena*, especially in its

organelles.

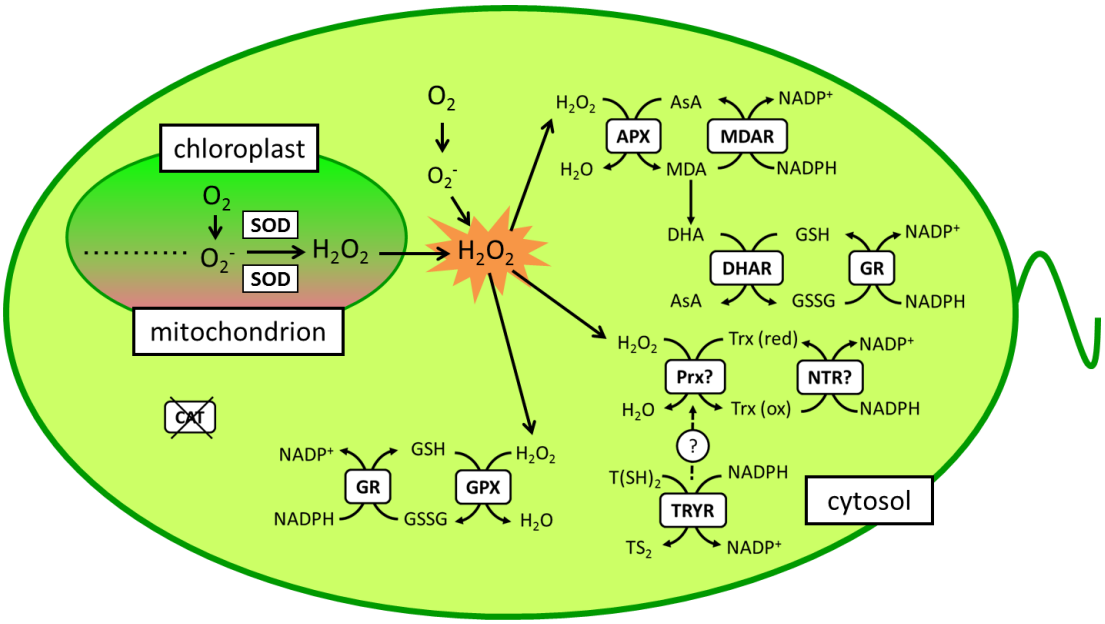

Figure I-2. Proposed ROS metabolic pathways in *Euglena* cells. AsA, ascorbate; CAT, catalase; DHA, dehydroascorbate; GSH, reduced glutathione; GSSG, oxidized glutathione; MDA, monodehydroascorbate; SOD, superoxide dismutase; Trx (ox), oxidized thioredoxin; Trx (red), reduced thioredoxin; TS_2, oxidized trypanothione; $T(SH)_2$, reduced trypanothione. Prx and enzymes consisting of Trx system have not yet been identified. It remains unclear that whether TRYR involves in ROS metabolism in *Euglena* cells.

In this study

To obtain the full-length cDNA sequences of expression genes in *Euglena*, our research group recently performed *Euglena* transcriptome analysis using de novo RNA-Seq method (Ishikawa et al., unpublished data). By a homology search of *Euglena* RNA-Seq data, I obtained genetic information on enzymes involved in thiol-based redox metabolism including Prxs, NTRs, GR, and TRYR. From the viewpoint of ROS metabolism and redox regulation in *Euglena* cells, it is crucial to understand that whether these enzymes function as antioxidative components and redox regulators, and whether both GSH and $T(SH)_2$ systems is physiologically functional in *Euglena* cells. In the present thesis, I studied the following aspects:

1. Identification and functional analysis of peroxiredoxin isoforms in *Euglena gracilis* (**CHAPTER II**)
2. Biochemical and physiological analyses of NADPH-dependent thioredoxin reductase isozymes in *Euglena gracilis* (**CHAPTER III**)
3. Comparative and functional analyses of glutathione reductase and trypanothione reductase in *Euglena graclis*. (**CHAPTER IV**)

CHAPTER II

Identification and functional analysis of peroxiredoxin isoforms in *Euglena gracilis*

Introduction

Reactive oxygen species (ROS) including superoxide, H_2O_2, and other free radical molecules are known to be the by-products of aerobic metabolism and cause oxidative damage to cells. In addition to this cytotoxic effect, ROS are important second messengers that regulate growth, development, and stress responses in various organisms (Mittler et al., 2004; Foyer and Noctor, 2005; Foyer and Shigeoka, 2011). Therefore, intracellular levels of ROS concentrations must be tightly controlled.

Photosynthetic organisms have developed various non-enzymatic and enzymatic systems to withstand oxidative damage and/or modulate ROS-induced oxidative signaling. The main ROS-scavenging enzymes of plants include superoxide dismutase, ascorbate peroxidase (APX), catalase, and peroxiredoxin (Prx). Even though plants have orthologous genes for glutathione peroxidase (GPX), these have been classified as a novel clade of Prx family because of their donor specificity (Rouhier and Jacquot, 2005; Iqbal et al., 2006). These enzymes have been identified in almost every subcellular compartment in higher plants, including the cytosol, chloroplasts, mitochondria, and peroxisomes (Mittler et al., 2004). These ROS-scavenging pathways have been shown to modulate the steady-state levels of ROS in different cellular compartments for signaling purposes as well as protection against oxidative damage.

The ROS-scavenging system of a photosynthetic protist, *Euglena gracilis*, has been shown to differ from that of plants (Shigeoka et al., 2002). *Euglena* lacks catalase, and contains a single APX, which is localized exclusively in the cytosol, but not in any other organelle (Shigeoka et al., 1980). Unlike APXs in higher plants, APX in *Euglena* consists of two entirely homologous catalytic domains, forms an intramolecular dimeric structure, and can reduce alkyl hydroperoxides as well as H_2O_2 (Ishikawa et al., 2010). We previously demonstrated that silencing APX expression in *Euglena* cells resulted in a significant increase in cellular H_2O_2 levels, which indicated its

physiological importance in the regulation of H_2O_2 levels. Enzymatic activities that comprise the ascorbate (AsA)-glutathione (GSH) cycle, including monodehydroascorbate reductase, dehydroascorbate reductase, and GSH reductase, have also only been found in the cytosol (Shigeoka et al., 1987a). Although *Euglena* contains non-selenium GPX, which uses reduced GSH as an electron donor (Overbaugh and Fall, 1985), the gene encoding GPX has not yet been identified. Therefore, because the identities of other ROS-metabolic enzymes have not yet been determined, ROS metabolism in *Euglena* cells, especially in its organelles, remains unclear.

Prxs constitute a family of thiol-based peroxidases found in all biological kingdoms from bacteria to plants and animals. Prxs have been classified into four types based on their structural and catalytic properties; 1-CysPrx, 2-CysPrx, type II Prx (PrxII), and PrxQ (Wood et al., 2003). 2-CysPrx, PrxII, and PrxQ contain two catalytic Cys residues, which are essential for the reduction of peroxides. During the catalytic cycle, one Cys residue is oxidized to sulfenic acid, whereas H_2O_2 and alkyl hydroperoxides are reduced to water or their corresponding alcohols. The oxidized Cys residue forms a disulfide bridge with the other Cys residue, which is then resolved by thioredoxin (Trx).

As for physiological importance of ROS-metabolic enzymes in higher plants, it has genetically revealed by several research groups. Tobacco plants overexpressing thylakoid membrane-bound APX (tAPX) showed increased tolerance to oxidative stress and chilling stress under high light condition (Yabuta et al., 2002). Furthermore, it has revealed by a conditional expression system for *Arabidopsis* tAPX that the enzyme plays a key role in controlling some gene expression levels in response to cellular redox status (Maruta et al., 2012). In addition to APX, *Arabidopsis* mutants deficient in 2-CysPrx had significantly higher H_2O_2 levels in their leaves, which supported the protective role of Prx in oxidative stress (Pulido et al., 2010). *Arabidopsis* mutants deficient in one of the GPX isoforms, AtGPX3 and AtGPX8, were shown to be sensitive to oxidative stress (Miao et al., 2006; Gaber et al., 2012). These findings suggest that Prxs and GPXs are important components of ROS scavenging in photosynthetic organisms as well as APXs. Furthermore, Prxs were shown to not only modulate cellular ROS-dependent signaling, but also, depending on

the Prx type, sense the redox state, transmit redox information to binding partners, and function as a chaperone (Dietz, 2011). The multiple functions of Prxs support their physiological importance in redox regulation and the stress response.

We recently performed RNA-seq analysis and identified a series of *Euglena* full-length cDNA sequences (Ishikawa et al., unpublished data). Although genetic information on ROS metabolic enzymes in *Euglena* has been limited, except for APX, at least four genes encoding putative Prx proteins (EgPrx1 ~ 4) have been identified by a BLAST search of the data, suggesting that Prxs are involved in ROS metabolism and redox regulation in *Euglena* cells as well as other organisms. I here examined the enzymatic properties of the Prx isoforms and demonstrated that their recombinant proteins could reduce H_2O_2 and alkyl hydroperoxides. I also investigated the effect of the knock down (KD) of EgPrxs on cell growth, and discussed the physiological role of EgPrx isoforms in ROS metabolism in *Euglena* cells.

Materials and Methods

Cell culture.

Euglena gracilis, strain Z, was maintained by regular subculturing and was grown in heterotrophic Koren–Hutner (KH) medium (Koren and Hutner, 1967) under continuous illumination (50 $\mu mol \cdot m^{-2} \cdot s^{-1}$) at 22 °C for 6 days, by which time the stationary phase was reached. Cells were grown in Cramer-Myers (CM) medium for autotrophic growth (Cramer and Myers, 1952). Cell number was counted using an electric field multi-channel cell counting system, CASY (Roche Diagnostics).

Cloning of cDNA encoding Euglena Prxs, and Trx and NADPH dependent Trx reductase (NTR) from yeast.

Full-length cDNA encoding mature *Euglena* Prx proteins was amplified by PCR with primers (Prx1-F, 5’-TTCTCGAGCCAGCAACTGTGCAGCATCC-3’; Prx1-R, 5’-AACTGCAGCTGTATGGGAACACCCGATAAC-3’; Prx2-F, 5’-GAGCTCTCGGCGTTCGTCGGAACC-3’; Prx2-R, 5’-AAGCTTCAGGCGTCCCACTTAGATTGCC-3’; Prx3-F, 5’-CATATGTCAACAAAAGCCTTCGTTC-3’; Prx3-R,

5’-GGATCCTCAATTCTTGTAGGTCTTG-3’; Prx4-F, 5’-CATATGGCCGTCGTGGACC-3’; Prx4-R, 5’-GGATCCTTACCCTTCGAAGGC-3’). The amplified fragments were cloned into a pGEM-T easy vector (Promega) to confirm the absence of PCR errors. The plasmids were digested with *Xho* I and *Pst* I for Prx1, *Sac* I and *Hind* III for Prx2, *Nde* I and *Bam* HI for Prx3 and Prx4, and the resulting DNA fragments were ligated into a pCold II vector (Takara) to produce His_6-tagged recombinant proteins. The *Escherichia coli* strain BL21 Star (Agilent Technologies) was used as a host for the expression of recombinant proteins. Full-length cDNA encoding Trx (accession number YGR209C) and NTR (accession number YDR353W) from yeast was amplified by PCR with primers (ScTrx-F, 5’-GAGCTCATGGTCACTCAATTAAAATC-3’; ScTrx-R, 5’-AAGCTTCTATACGTTGGAAGCAATAG-3’; ScNTR-F, 5’-GAGCTCATGGTTCACAACAAAG-3’; ScNTR-R, 5’-AAGCTTGCTATTCTAGGGAAGTTAAG-3’), and finally subcloned into pCold II vector as well as the procedures for *EgPrxs*. The resulting constructs were transformed into *E. coli* BL21 Star.

Expression and purification of recombinant proteins.

Transformed cells were grown in LB medium supplemented with 50 $\mu g \cdot mL^{-1}$ ampicillin at 37 °C. When the culture reached an absorbance of 0.4–0.5 at 600 nm, 0.5 mM isopropyl β-D-thiogalactopyranoside was added, and the cells were grown further at 15 °C for 20 h. *E. coli* cells were resuspended in 20 mM HEPES-NaOH buffer, pH 7.0, and lysed by sonication. His-tagged recombinant proteins were purified on a column packed with TALON Metal Affinity resin (Clontech). Finally, the purified enzymes were desalting and concentrated using an ultrafiltration membrane (Amicon® Ultra-4, Millipore), and stored at -20 °C until used.

Crude extract from Euglena cells.

Euglena cells were collected by brief centrifugation and suspended in three volumes of an ice-cold buffer (HEPES-NaOH, pH 7.0) and disrupted by sonication. The cell lysate was centrifuged at 40,000 rpm at 4 °C for 30 min and the supernatant was used for the assay of Prx activity. For the assay of APX and GPX activities, buffer was

replaced with 50 mM potassium phosphate, pH 7.0, containing 1 mM EDTA and 1 mM AsA and 50 mM potassium phosphate, pH 7.0, respectively.

Enzyme assays.

Trx-dependent peroxidase activity was measured as the decrease in absorbance at 340 nm (ε = 6.22 mM^{-1} cm^{-1}) due to NADPH oxidation according to Kim et al. (2010). The reaction mixture contained 0.2 mM NADPH, 6 μM Trx, 0.3 μM Trx reductase, and 0.1 mM H_2O_2 in 20 mM HEPES-NaOH, pH 7.0, in a final volume of 0.1 mL. The reaction mixture was preincubated for 1 min and started by the addition of H_2O_2. NADPH consumption was monitored by the decrease in absorbance at 340 nm for 1 min. AsA-dependent peroxidase activity was measured as the decrease in absorbance at 290 nm (ε = 2.8 mM^{-1} cm^{-1}) due to AsA oxidation according to Ishikawa et al. (2010). The reaction mixture contained 1 mM EDTA, 0.4 mM AsA, and 0.1 mM H_2O_2 in 50 mM potassium phosphate buffer, pH 7.0, in a final volume of 1 mL. GSH-dependent peroxidase activity was measured as the decrease in absorbance at 340 nm due to NADPH oxidation. The reaction mixture contained 0.2 mM NADPH, 2 mM GSH, 1 U GSH reductase, and 0.1 mM H_2O_2 in 50 mM potassium phosphate buffer, pH 7.0, in a final volume of 1 mL. The activity of each peroxidase with organic peroxides was also assayed using the same reaction mixture; however, H_2O_2 was replaced with 0.1 mM *t*-butyl hydroperoxide or 0.1 mM cumene hydroperoxide.

RNA isolation and quantitative PCR analysis.

Total RNA was isolated from *Euglena* cells using RNAiso (Takara). Briefly, *Euglena* cells were homogenized in 1 mL of RNAiso followed by chloroform extraction at 13,000 rpm for 20 min. RNA in the supernatant was precipitated with an equal volume of isopropanol and washed with 70% ethanol. Total RNA was purified with a NucleoSpin® RNA Plant (Takara) according to the manufacturer's instructions and quantified with Nanodrop 1000 (Thermo Fisher Scientific). A 500 ng aliquot of purified RNA was used for cDNA synthesis using PrimeScript RT Master Mix (Takara) according to the manufacturer's instructions. The cDNA synthesized was then used in real-time PCR with forward and reverse primers specific for each of the genes analysed: EF1α-F, 5'-ACAGATTGGGAACGGGTACGC-3'; EF1α-R,

5’-TTCATCAGGACAATCGCAGCA-3’; Prx1-F, 5’-GAAGTGTGTCCGGCAAAC-3’; Prx1-R, 5’-AAGCTGTATGGGAACACCC-3’; Prx2-F, 5’-TGGGACGCCTGTTTTATC-3’; Prx2-R, 5’-CAAAGAATGCCTCCGTG-3’; Prx3-F, 5’-CCTGCCAACTGGACACC-3’; Prx3-R, 5’-ACCATCCACCAGCATGC-3’; Prx4-F, 5’-TTCGAAGGGTAACCCGC-3’; Prx4-R, 5’-AGTCCTGTGAATCAGCCTG-3’; APX-F, 5’-GCACGACGCTGGCACATACG-3’ and APX-R, 5’-AATGTCGAGGCCGTTGTTGGAG-3’. Real-time PCR was performed with SYBR Premix Ex Taq (Takara) on the Thermal Cycler Dice Real Time System TP850 (Takara).

RNA interference (RNAi) experiments.

Silencing of Prx by RNAi was performed as described previously (Ishikawa et al., 2010). An approx. 500-bp partial *Euglena* Prx cDNA was PCR-amplified with the addition of the T7 RNA polymerase promoter sequence (underlined in the primer sequences below) at one end. The primers were Prx1/RNAi-F (5’-TAATACGACTCACTATAGGGTCAACGGGGAGTTCAAG-3’), Prx1/RNAi-R (5’-TAATACGACTCACTATAGGGGGGATCTGCCTTCATCG-3’), Prx2/RNAi-F (5’-TAATACGACTCACTATAGGGAGTGACCGTGCTGCC-3’), Prx2/RNAi-R (5’-TAATACGACTCACTATAGGGCCTTGCTTCCGACTGG-3’), Prx3/RNAi-F (5’-TAATACGACTCACTATAGGGCAACCTTGCGTCCATATTC-3’), Prx3/RNAi-R (5’-TAATACGACTCACTATAGGGCACGAATTGGAAAGCAGAG-3’), Prx4/RNAi-F (5’-TAATACGACTCACTATAGGGTACCGCTGGCAGGAC-3’) and Prx4/RNAi-R (5’-TAATACGACTCACTATAGGGGGCGTCCGACACCTC-3’). Sense and antisense RNAs were synthesized using the PCR products as templates (MEGAscript RNAi Kit; Life Technologies). After purification of the transcribed RNA with DNase I digestion followed by ethanol precipitation, double-stranded RNA (dsRNA) was produced by annealing equimolar amounts of the sense and antisense RNAs. *Euglena* cells from 2-day-old cultures were collected and resuspended in KH medium. The cell suspension (100 μL; approx. 1×10^7 cells) was transferred to a 0.2-cm-gap cuvette and electroporated with 15 μg of Prx-dsRNAs using NEPA21 (NEPA GENE). The cell suspension was diluted with fresh KH medium and cultured at 22 °C for restoration.

Spot assay.

The cell growth rates of control and silencing cells were determined with spot assays. Cultures of each cell were spotted onto KH (heterotrophic) and CM (autotrophic) plates. The numbers of cells spotted were 4×10^4 (1), 2×10^4 (1/2), 1×10^4 (1/4), 5×10^3 (1/8), and 2.5×10^3 (1/16). Cells were grown under continuous illumination (50 $\mu mol \cdot m^{-2} \cdot s^{-1}$) at 22 °C for 5 days and pictures were taken.

Results and Discussion

Primary sequence of four Euglena Prxs

I obtained genetic information on four full-length cDNAs encoding Prx by a tblastn search of our RNA-seq data constructed recently (Ishikawa *et al.*, unpublished data). These genes were designated as *EgPrx1 ~ 4* (accession number AB853312, AB853313, AB853314, and AB853315, respectively). The cDNA sequences of all *EgPrxs*, except for *EgPrx3*, contained a spliced leader sequence, a characteristic motif of *Euglena* transcripts generated by *trans*-splicing manner at their 5' end (Tessier et al., 1991), indicated that these cDNA sequences were obtained as full-length cDNA. As for *EgPrx3*, the first ATG codon appeared following predicted 5' UTR region, indicating that the clone definitely contained full-length protein coding region.

Homology analysis indicated that EgPrx1, -2, and -3 were highly identical to each other (approx. 57-83% identity), whereas EgPrx4 had low identity (approx. 22-36% identity) with the other EgPrxs (**Table II-1**). These results suggested that EgPrx1, -2, and -3 belonged to the same subgroup, but were distinct from EgPrx4. To reveal the classification of four EgPrxs, the identities of EgPrxs with known Prxs including all Prx subgroups were determined. Prx1, -2, and -3 were highly identical (approx. 48-75%) to 2-CysPrxs from various organisms such as mammals, plants, algae, and trypanosomatids, whereas EgPrx4 was approx. 45-69% identical to PrxII from algae and plants (**Table II-1**). In contrast, these Prxs had low identities (approx. 20-30% identity) to Prxs in the other subclass. Thus, EgPrx1, 2, and 3 may be classified as 2-CysPrx and EgPrx4 as PrxII.

Table II-1. Homology analysis of *Euglena* Prxs with Prxs from various organisms. The values represent the percent identities calculated *Euglena* Prxs to each other and with Prxs from various organisms.

Organism	Enzyme	Identity (%)			
		EgPrx1	EgPrx2	EgPrx3	EgPrx4
Euglena gracilis	Prx1	—	60	83	22
	Prx2	60	—	57	36
	Prx3	83	57	—	22
	Prx4	22	36	22	—
Homo sapiens	Prx1	65	59	65	28
	Prx2	69	59	64	27
	Prx5	30	30	24	42
Mus musculus	Prx5	31	26	23	39
Arabidopsis thaliana	2CPA	60	69	48	25
	2CPB	58	70	58	26
	PrxIIC	35	25	35	45
	PrxIIE	19	25	21	46
Chramydomonas reinhardtii	Prx1	61	75	53	30
	Prx3	24	23	25	45
	Prx5	26	29	25	52
Synechocystis sp. PCC6803	2CP	55	65	56	26
	PrxII	24	35	25	69
Trypanosoma brucei	CTXNPx	65	55	67	23
Leishmania major	TryP1	60	49	60	20

The sequence alignments and phylogenetic tree of EgPrx1, -2, and -3 with the known 2-CysPrxs and EgPrx4 with the known PrxIIs were constructed using the ClustalW program. As shown in **Figure II-1**, all EgPrxs had two conserved Cys residues, which were essential for the catalytic reaction of 2-CysPrx and PrxII (Wood et al., 2003). All EgPrxs additionally contained conserved Pro, Thr, and Arg residues, which were important for catalytic Cys stability or peroxide reduction in the known 2-CysPrxs and PrxIIs (Wood et al., 2003). The phylogenetic tree indicated that EgPrx1 and EgPrx3 were very close to the protozoa clade including *Trypanosoma brucei* and

Leishmania major, while EgPrx2 and EgPrx4 were close to plants and the algae clade, such as *Synechocystis* sp. PCC6803 (**Figure II-2**).

A

```
EgPrx1    -----------------MPATVQHPAPDFDAVAVV-NGEFKNVKLSDYKG-KYVVLFFYP 41
EgPrx2    VSRYEA--AEQQWSMMAASAFVGTKAPAFKATAVY-DEEFVDIDLSDYKGKKYVVLFFYP 177
EgPrx3    ALRRSVPLSLSTLRPYSTKAFVQKPAPDFSATALV-NGEFKTVKLSDFRG-KYVVLFFYP 113
TbCTXNPx  --------------MSCGDAKLNHPAPHFNEVALMPNGTFKKVDLASYRG-KWVVLFFYP 45
S6803_2CP ---------------------VGQPAPDFTATAIV-DQSFQTVKLSTYRG-KYLVLFFYP 43
At2CPA    VK-----------AQADDLPLVGNKAPDFEAEAVF-DQEFIKVKLSDYIGKKYVILFFYP 112
HsPrx1    --------------MSSGNAKIGHPAPNFKATAVMPDGQFKDISLSDYKG-KYVVFFFYP 45
                               :   ** *   *:  :  *  :.*: : * *::::***

EgPrx1    LDFTFVCPTEIIAFNDAAPKFKEIGAELLAVSVDSQFSHLAWINTPRNKGGLGHMEIPLI 101
EgPrx2    LDFTFVCPTEITAFSDRAAEFEALDTQILGVSVDSQFSHLAWIQTPRNQGGLGEIKYPLV 237
EgPrx3    LDFTFVCPTEIIAFNDAAAKFKEANCELIALSVDSHFSHLAWVNTPRNKGGLGHMEIPIV 173
TbCTXNPx  LDFTFVCPTEICQFSDRVKEFNDVDCEVIACSMDSEFSHLAWTNVERKKGGLGTMNIPIL 105
S6803_2CP LDFTFVCPTEIIAFSDRHSEFTALDTEVVGISVDSEFSHLAWIQTERKMGGIGNINYPLV 103
At2CPA    LDFTFVCPTEITAFSDRHSEFEKLNTEVLGVSVDSVFSHLAWVQTDRKSGGLGDLNYPLI 172
HsPrx1    LDFTFVCPTEIIAFSDRAEEFKKLNCQVIGASVDSHFCHLAWVNTPKKQGGLGPMNIPLV 105
          *****:*****  *.*   :*   . :::. *:** *.**** :. :: **:* :: *::

EgPrx1    ADVTKQIAKDYGVLIEGAGVALRGLFIIDGEGKLRSMLINDLPVGRSVDETLRLVSAFQF 161
EgPrx2    ADLKKDIAEAYGVLTEDG-VALRGLFIIDKESVIQHATINNLAFGRNVDETLRVLEALQH 296
EgPrx3    ADITKQISKDYGVLIEEAGIALRGLFIIDGEGNIRSLTINDLPVGRSVEETLRLVSAFQF 233
TbCTXNPx  ADKTKSIMKAYGVLKEEDGVAYRGLFIIDPQQNLRQITINDLPVGRNVDETLRLVKAFQF 165
S6803_2CP SDLKKEISQAYNVLEPDAGIALRGLFIIDREGILQYATVNNLSFGRSVDETLRVLKAIRH 163
At2CPA    SDVTKSISKSFGVLIHDQGIALRGLFIIDKEGVIQHSTINNLGIGRSVDETMRTLQALQY 232
HsPrx1    SDPKRTIAQDYGVLKADEGISFRGLFIIDDKGILRQITVNDLPVGRSVDETLRLVQAFQF 165
          :* .: * : :.**     :: ******* :  ::   :*:* .**.*:**:* :.*::.

EgPrx1    TDKHG-EVCPANWKPGAATMKADPKGSQEYFSTVQ-- 195
EgPrx2    VQANPDEVCPAGWKKGDKTMKPDPVGSKEYFKAI--- 330
EgPrx3    VDKHG-EVCPANWTPGASTMKADPQGSQEFFSKTYKN 269
TbCTXNPx  VEKHG-EVCPANWKPGSKTMKADPNGSQDYFSSMN-- 199
S6803_2CP VQSHPNEVCPVDWQEGDKTMIPDPEKAKTYFETVAEP 200
At2CPA    IQENPDEVCPAGWKPGEKSMKPDPKLSKEYFSAI--- 266
HsPrx1    TDKHG-EVCPAGWKPGSDTIKPDVQKSKEYFSKQK-- 199
           : :  ***..*  *  :: .*   :: :*.
```

B

```
EgPrx4      ----MAVVDRVPDVVFKTRVRDDSIS-PNPYR--WQDTTTADLFAGKKVVVFSLPGAFTP 53
S6803_PrxII -----MTPERVPSVVFKTRVRDESVPGPNPYR--WEDKTTEQIFGGKKVVLFSLPGAFTP 53
CrPrx3      -----------MPIAVGDKVPAATFHVPDANG-MPQPLTTEQLFGGKKVLLFAVPGAYTP 48
AtPrxIIE    TRSFATTP-VTASISVGDKLPDSTLSYLDPSTGDVKTVTVSSLTAGKKTILFAVPGAFTP 119
HsPrx5      VRSFSRAAAAMAPIKVGDAIPAVEVFEGEPG----NKVNLAELFKGKKGVLFGVPGAFTP 98
                       : .   :    .   :.    :  .  .:  *** ::*.:***:**

EgPrx4      TCSSNHLPRYDELYDEFRALGVDQIICVSVNDAFVMFRWGRSLEVK-NLFLLPDGNGEIT 112
S6803_PrxII TCSSNHLPRYEQLFEEFQALGVDDIICLSVNDAFVMFQWGKQIGAD-KVKLLPDGNGEFT 112
CrPrx3      TCSKQHLPGFVESADALKAKGVDTIACLSVNDAFVMGAWGQSIGVGDKVTMLADGAAAFT 108
AtPrxIIE    TCSQKHVPGFVSKAGELRSKGIDVIACISVNDAFVMEAWRKDLGINDEVMLLSDGNGEFT 179
HsPrx5      GCSKTHLPGFVEQAEALKAKGVQVVACLSVNDAFVTGEWGRAHKAEGKVRLLADPTGAFG 158
            **. *:* : .    ::: *:: : *:******   * :      :: :*.*  . :

EgPrx4      RKMGMLVDKTN--IGFGMRSWRYSMLVTDGRIEKFFCEPGLADNAATDPFEVSDADTMLA 170
S6803_PrxII RKMGMLVEKSN--LGFGMRSWRYSMFVNDGKIEKMFIEPEFGDNCPVDPFECSDADTMLA 170
CrPrx3      KAVG--LDQDLSEAGLGVRSQRYAMLVEDGVVKVLNVEP-------ARGLTCSSAASMLE 159
AtPrxIIE    GKLGVELDLRDKPVGLGVRSRRYAILADDGVVKVLNLEE-------GGAFTNSSAEDMLK 232
HsPrx5      KETDLLLDDSLVSIFGNRRLKRFSMVVQDGIVKALNVEPD------GTGLTCSLAPNIIS 212
               .  ::        . *  *:::.. ** :: :  *          :  * *  ::

EgPrx4      YLKGQQPQGIATP-HAFEG 188
S6803_PrxII YLKGAEAPGVSEPVKAFVG 189
CrPrx3      GL----------------- 161
AtPrxIIE    AL----------------- 234
HsPrx5      QL----------------- 214
             *
```

Figure II-1. Amino acid sequence alignment of Prxs from *Euglena* and other organisms. Comparison of the predicted amino acid sequences of (A) *Euglena* Prx1, 2, and 3 with 2-CysPrxs from *Trypanosoma brucei* (TbCTXNPx), *Synechocystis* sp. PCC6803 (S6803_2CP), *Arabidopsis thaliana* (At2CPA), and *Homo sapiens* (HsPrx1) and (B) *Euglena* Prx4 with PrxII from *Synechocystis* sp. PCC6803 (S6803_PrxII), *Chlamydomonas reinhardtii* (CrPrx3), *A. thaliana* (AtPrxIIE), and *H. sapiens* (HsPrx5). Letters shown in white on a black background represent conserved catalytic Cys residues. The residues involved in catalytic Cys stability or peroxide reduction are shown in black letters on a grey background. The box shows the common motif LRR found in the presequence of Euglenozoa mitochondrial proteins. Asterisks indicate amino acids conserved in all sequences, and colons and dots indicate amino acids with similar biochemical characteristics.

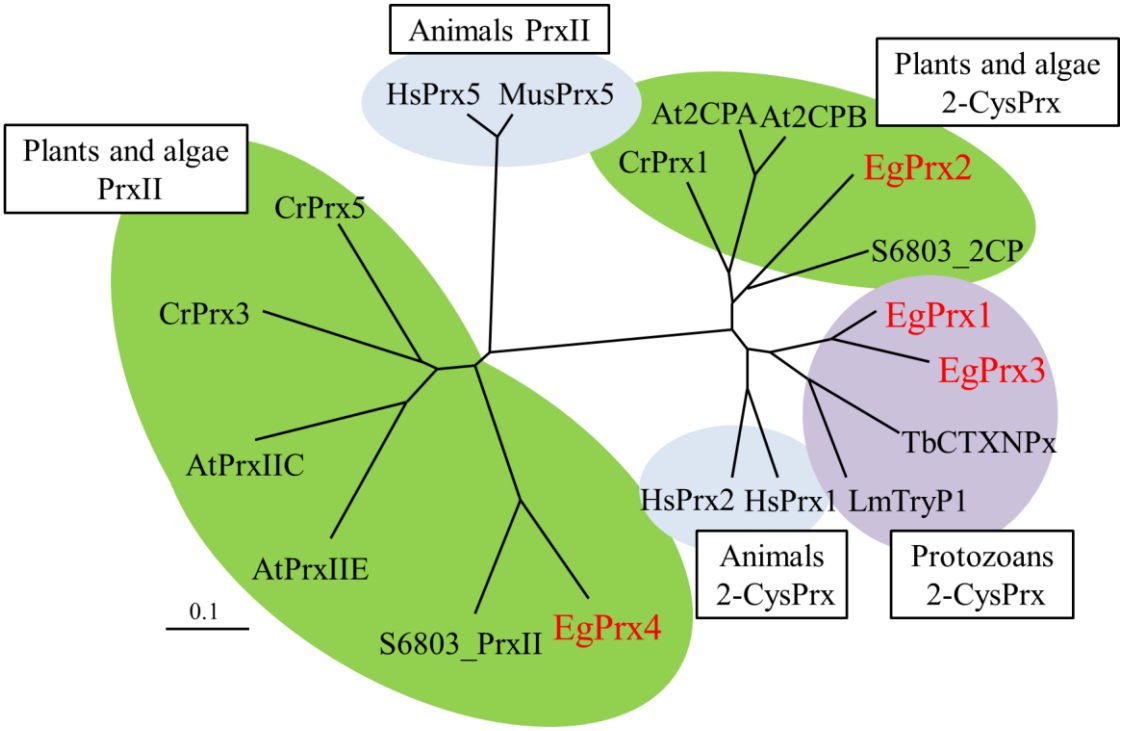

Figure II-2. Phylogenetic tree for Prxs from *Euglena* and other organisms. The phylogenetic tree was constructed using the ClustalW program and visualized with TreeView. Abbreviations and UniProt accession numbers for the 2-CysPrx and PrxII orthologues are as follows: Hs, *Homo sapiens* (HsPrx1, Q06830; HsPrx2, P32119; HsPrx5, P30044); Mus, *Mus musculus* (MusPrx5, P99029), At, *Arabidopsis thaliana* (At2CPA, Q96291; At2CPB, Q9C5R8; AtPrxIIC, Q9SRZ4; AtPrxIIE, Q949U7); Cr, *Chlamydomonas reinhardtii* (CrPrx1, D5L2X1; CrPrx3, A8HZQ4; CrPrx5, A8HPG8); S6803, *Synechocystis* sp. PCC6803 (S6803_2CP, Q55624; S6803_PrxII, P73728); Tb, *Trypanosoma brucei* (TbCTXNPx, Q71RY2); and Lm, *Leishmania major* (LmTryP1, Q4QF80).

Each amino acid sequence was analyzed using TMHMM (http://www.cbs.dtu.dk/services/TMHMM/) and TargetP (http://www.cbs.dtu.dk/services/TargetP/) programs to predict the subcellular localization of EgPrxs. The TMHMM program revealed that two transmembrane domains existed at the N-terminal region of EgPrx2 (**Figure II-3B**), corresponding to a typical transit signal motif for plastid-targeted proteins in *Euglena* (Durnford and Gray, 2006). Thus, EgPrx2 may be localized in plastids. Because *Euglena* plastids are surrounded by a lipid trilayer and the protein import mechanism into plastids differs from that of typical plant plastids (Sláviková et al., 2005), it is difficult to predict exact *Euglena* plastid signals using the TargetP program. In contrast, the TargetP program predicted the existence of a 25 amino acid mitochondrial targeting peptide at the N-terminal region of EgPrx3 (**Figure II-3E**). Additionally, the N-terminal region of EgPrx3 contained a common LRR motif found in the presequence of Euglenozoa mitochondrial proteins (**Figure II-1A**) (Krnáčová et al., 2012). These findings indicated that EgPrx3 was localized in mitochondria. Both programs indicated that EgPrx1 and EgPrx4 had no characteristic signal motif (**Figure II-3A, D and E**), which suggested that they were cytosolic enzymes. Therefore, the EgPrx1 and EgPrx4 isoforms consisted of 195 and 188 amino acids with calculated molecular masses of 21.3 and 21.1 kDa, respectively. The predicted mature Prx2 and Prx3 isoforms were 194 and 198 amino acids with 21.5 and 21.8 kDa, respectively.

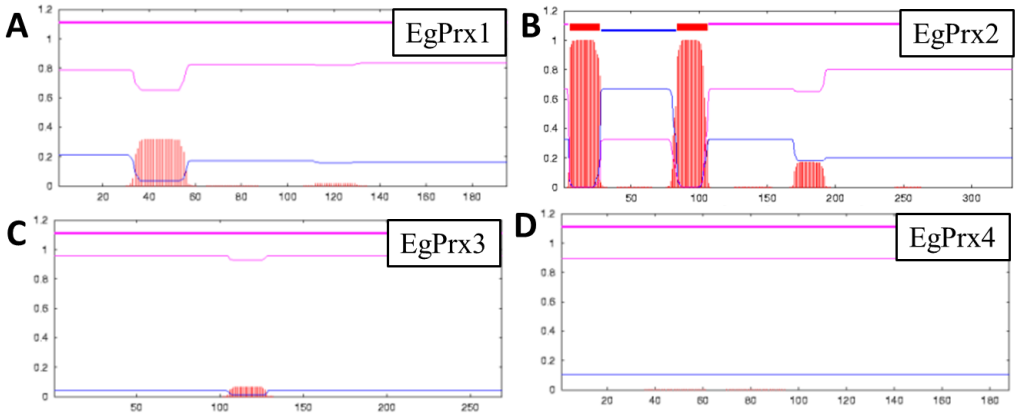

E

	cTP	mTP	SP	other	Loc	RC	Tplen
EgPrx1	0.018	0.090	0.163	0.964	—	1	—
EgPrx2	0.010	0.057	0.833	0.117	S	2	29
EgPrx3	0.066	0.897	0.016	0.014	M	1	25
EgPrx4	0.038	0.131	0.120	0.872	—	2	—

Figure II-3. Prediction of the subcellular localization of *Euglena* Prxs. (A-D) Prediction of the transmembrane regions of EgPrxs using the TMHMM program. (E) Prediction of the subcellular localization of EgPrxs using the TargetP program. cTP, mTP, and SP represent the possible values of chloroplast transit peptide (cTP), mitochondrial targeting peptide (mTP), and secretory pathway signal peptide (SP), respectively. Loc represents the prediction of localization; S and M mean secretory pathway and mitochondrion, respectively. RC represents the reliability class, from 1 to 5, in which 1 indicates the strongest prediction. Tplen represents the predicted presequence length.

Although two 2-CysPrxs were shown to be localized exclusively in chloroplasts in *Arabidopsis* (Dietz et al., 2006), two 2-CysPrxs may also be localized in the cytosol and chloroplasts of *Chlamydomonas* (Dayer et al., 2008). Trypanosomatids, belonging to the protist phylum Euglenozoa as well as *Euglena*, were shown to contain 2-CysPrxs in the cytosol and mitochondria (Castro and Tomás, 2008). The existence of putative cytosolic, chloroplastic, and mitochondrial 2-CysPrxs

in *Euglena* has been suggested in this study, which is close to the constitution of *Chlamydomonas* or Trypanosomatids, but not of plants. Although genes encoding PrxQ were identified in cyanobacteria, plants, and *Chlamydomonas* (Dietz, 2011), whether *Euglena* contained PrxQ could not be determined in this study.

Enzymatic properties of recombinant Euglena Prxs

To reveal the enzymatic properties of EgPrxs, each recombinant EgPrx (rEgPrx) protein was expressed in *E. coli* and purified to homogeneity, as judged by SDS-PAGE (**Figure II-4A**). Since the *E. coli* Trx/NTR system is often used for general Prx activity assays, I attempted to determine the activity of rEgPrx1 using this system. However, Trx-dependent peroxidase activity was not detectable (data not shown). This may have been due to the weaker affinity of EgPrxs for *E. coli* Trx, which suggested a conformational difference between EgPrxs and the other known Prxs. Human Prx1 was previously shown to exhibit higher activity with the yeast system than with the *E. coli* system (Kim et al., 2005). Thus, I prepared purified recombinant Trx and NTR from yeast (*Saccharomyces cerevisiae*) (**Figure II-4B**). The Prx activities of all rEgPrxs were determined using the yeast Trx/NTR system (**Table II-2**). Thus, I used the yeast system for the following assay.

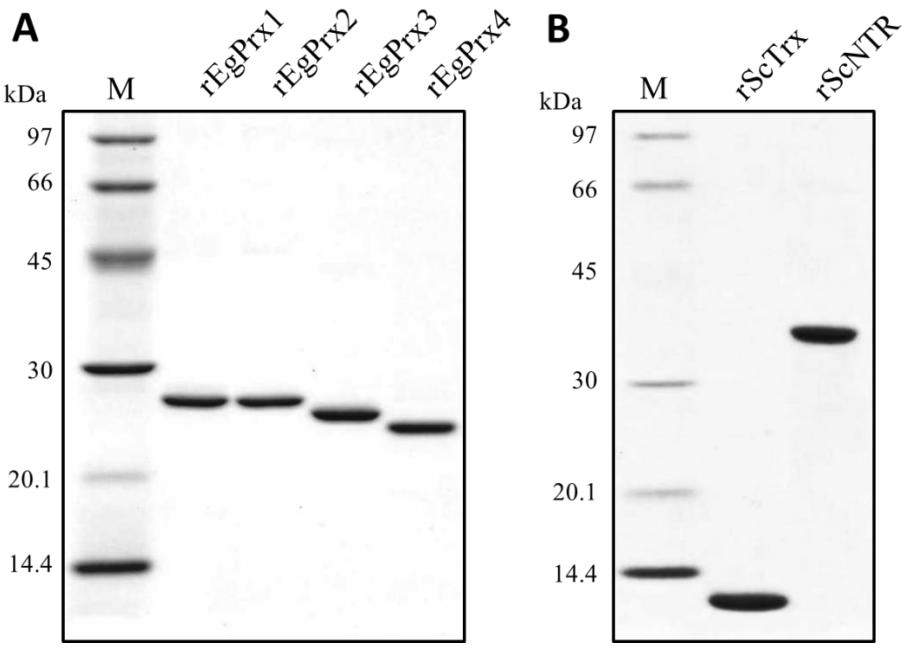

Figure II-4. SDS-PAGE of Purified Recombinant *Euglena* Prxs (A) and Yeast Trx and NTR (B). Recombinant His_6-tagged proteins were extracted from *E. coli* BL21 Star cells transformed with pColdII containing (A) the mature *Euglena* Prx1 (rEgPrx1), Prx2 (rEgPrx2), Prx3 (rEgPrx3), and Prx4 (rEgPrx4), (B) yeast Trx (rScTrx) and NTR (rScNTR), and were then purified using a TALON® Metal Affinity resin. The samples were separated by SDS-PAGE and stained with Coomassie Brilliant Blue.

Table II-2. Peroxide specificities of recombinant *Euglena* Prxs. The Prx activities of recombinant enzymes to 100 μM H_2O_2, *t*-butylhydroperoxide (*t*-BOOH) and cumene hydroperoxide (Cumene-OOH) were assayed using Yeast Trx and NTR as a reducing agent. Values are the mean ± SD (n = 3). n.d.; not detectable.

Substrate	Specific activity			
	rEgPrx1	rEgPrx2	rEgPrx3	rEgPrx4
	(μmol min^{-1} mg^{-1} protein)			
H_2O_2	2.11±0.05	2.08±0.08	1.49±0.15	0.42±0.13
t-BOOH	1.66±0.01	2.01±0.03	0.94±0.04	0.46±0.01
Cumene-OOH	0.80±0.13	1.16±0.14	0.25±0.03	n.d.

To examine the substrate specificity of rEgPrxs, enzyme activities were measured using H_2O_2, *ter*-butylhydroperoxide (*t*-BOOH), and cumene hydroperoxide (cumene-OOH) as substrates. As shown in **Table II-2**, all rEgPrxs, except for rPrx4, catalyzed the reduction of all substrates with activities of 0.25-2.11 μmol min^{-1} mg^{-1} protein. rEgPrx4 could reduce H_2O_2 and *t*-BOOH, but not cumene-OOH. Therefore, *Euglena* Prxs could reduce both H_2O_2 and alkyl hydroperoxide. Barley 2-CysPrx reduced *t*-BOOH and cumene-OOH at almost the same rates as H_2O_2 (König et al., 2002). *Leishmania donovani* TXNPx reacted with H_2O_2, *t*-BOOH, cumene-OOH, linolic acid hydroperoxide, and phosphatidyl choline hydroperoxide (Flohé et al., 2002). Therefore, the broad substrate specificities of EgPrxs were consistent with those of the known Prxs.

A kinetic analysis of rEgPrxs was then performed. As shown in **Table II-3**, the V_{max}, K_m, and k_{cat} values of rEgPrx1 for H_2O_2 were 3.15 μmol min^{-1} mg^{-1} protein, 39.1 μM, and 1.21 s^{-1}. The catalytic efficiency (k_{cat}/K_m) of rEgPrx1 for H_2O_2 was 3.1×10^4 M^{-1} s^{-1}. The kinetic parameters of rEgPrx2 and rEgPrx3 for H_2O_2 were similar to those of rEgPrx1. Although the K_m value of rEgPrx4 for H_2O_2 was 10-fold lower than that of the other EgPrx isoforms, the V_{max} and k_{cat} values of rPrx4 were 4 to 6-fold lower than those of the other Prx isoforms, which indicated that their catalytic efficiencies were

nearly equal to each other. The kinetic parameters of these enzymes for *t*-BOOH and cumene-OOH were similar to those of H_2O_2. Previous studies reported that the catalytic efficiencies of 2-CysPrx from pea and barley were 2.5×10^4 and 1.1×10^5 M^{-1} s^{-1}, respectively (Bernier-Villamor et al., 2004; König et al., 2003). Plant GPX isoforms were able to reduce H_2O_2 and alkyl hydroperoxides using Trx, but not GSH (Iqbal et al., 2006; Navrot et al., 2006). The k_{cat}/K_m values of *Arabidopsis* GPX1, 2, 5, and 6 for H_2O_2 were 4.9×10^3, 4.5×10^3, 3.1×10^3,and 6.1×10^3 M^{-1} s^{-1}, respectively (Iqbal et al., 2006). Thus, the catalytic efficiencies of the rEgPrxs were similar to those of the plant Prxs and GPXs, which suggested that *Euglena* Prxs functioned as a peroxidase as well as plant enzymes. However, the k_{cat} value and catalytic efficiency of *Euglena* recombinant APX for H_2O_2 were markedly higher than those of rEgPrxs (577 s^{-1} and 1.65×10^7 M^{-1} s^{-1}, respectively) (Ishikawa et al., 2010). While I was unable to accurately compare the activity of Prx with that of APX because of electron donor differences between the heterologous Trx/NTR system and AsA, APX may be an efficient peroxidase for cytosolic H_2O_2 metabolism in *Euglena* cells.

Table II-3. Kinetic parameters of recombinant *Euglena* Prxs. The activity assay was performed using concentrations of 2 to 100 μM of the peroxide substrates. Each rEgPrx was added at a concentration of 1 μM. Values are the mean ± SD (n = 3).

	Substrate	V_{max} (μmol min^{-1} mg^{-1} protein)	K_m (μM)	k_{cat} (s^{-1})	k_{cat} / K_m (M^{-1} s^{-1})
rEgPrx1	H_2O_2	3.15±0.34	39.1±4.1	1.21±0.13	3.1×10^4
	t-BOOH	2.21±0.21	24.5±4.9	0.85±0.08	3.5×10^4
	Cumene-OOH	1.73±0.09	24.6±2.5	0.66±0.03	2.7×10^4
rEgPrx2	H_2O_2	3.34±0.51	44.7±3.1	1.28±0.19	2.9×10^4
	t-BOOH	2.92±0.13	38.8±1.8	1.12±0.05	2.9×10^4
	Cumene-OOH	2.71±0.05	37.7±3.0	1.04±0.02	2.8×10^4
rEgPrx3	H_2O_2	2.29±0.16	37.8±6.5	0.88±0.06	2.3×10^4
	t-BOOH	2.22±0.11	36.1±2.6	0.85±0.04	2.4×10^4
	Cumene-OOH	1.33±0.08	22.2±3.0	0.51±0.03	2.3×10^4
rEgPrx4	H_2O_2	0.59±0.04	3.4±0.5	0.22±0.01	6.6×10^4
	t-BOOH	0.77±0.09	12.1±1.4	0.29±0.04	2.4×10^4

Expression analysis of Euglena peroxidases

The steady-state transcripts of *EgPrx1 ~ 4* and *EgAPX* were detected in *Euglena* cells grown heterotrophically under normal growth conditions. Quantitative PCR analysis revealed that the transcript levels of *EgPrx1*, *-2*, and *-3* were significantly higher than those of *EgAPX*, whereas those of *EgPrx4* were very low (**Figure II-5**). In general, Prx is known to accumulate to high concentrations. For example, *Arabidopsis* 2-CysPrxs have been shown to be among the top 20 most abundant stromal proteins (Peltier et al., 2006). König et al. (2002) estimated the stromal 2-CysPrx concentration to be 60 μM. The high transcript levels of *EgPrxs* and these findings suggest that EgPrxs also exist abundantly in each compartment. The lower catalytic efficiencies of EgPrxs than that of EgAPX may be compensated for by their higher abundance.

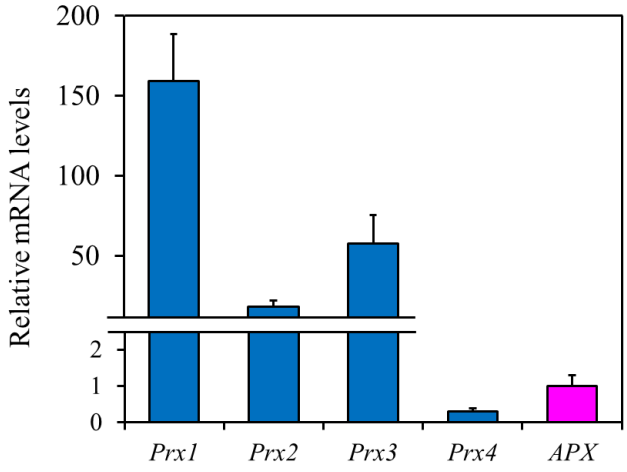

Figure II-5. Expression of *Prx* and *APX* genes in *Euglena*. Total RNA was extracted from 7-d-old *Euglena* cells grown heterotrophically under normal growth conditions and was converted into first-strand cDNA using an oligo dT primer. Quantitative PCR analysis was performed to determine the expression levels of *Prx1*, *2*, *3*, and *4* and *APX*. Relative amounts were normalized to *EF1α* mRNA. Values are the mean ± SD (n=3).

However, total Prx activity for H_2O_2 in crude extracts from *Euglena* cells grown under the same conditions was 15% that of APX activity (**Table II-4**). Prx activities for other substrates were similar to that of APX activity. Total GPX activities for all substrates were similar to that of Prx activity. In *Arabidopsis*, APX activity for H_2O_2 in leaf extracts was 7-fold higher than that of Trx-dependent peroxidase activity (Dietz et al., 2006), which correlated with the results of *Euglena*. The susceptibility of plant chloroplastic APX isoforms to oxidative inactivation in the absence of AsA explains the contribution of Prx to H_2O_2 reduction in the chloroplasts (Yabuta et al., 2002). The activity and protein of APX were detected in the cytosol only of *Euglena*, and not in the organelles including chloroplasts and mitochondria (Ishikawa et al., 2010). Moreover, *Euglena* RNA-Seq analysis suggested the existence of NTRC, which is the fusion protein of the NTR and Trx module found in the chloroplasts, and the mitochondrial Trx/NTR system in *Euglena* cells (data not shown). Therefore, EgPrx2 and -3 may contribute to ROS metabolism in the chloroplasts and mitochondria of *Euglena* cells, respectively.

Table II-4. Peroxidase activities in extracts from *Euglena* cells. Peroxidase activities were measured using 6 μM Trx and 0.3 μM NTR from yeast for Prx activity, 0.4 mM AsA for APX activity, and 2 mM GSH and 1 U/mL GSH reductase from yeast for GPX activity. Each peroxide was added at a concentration of 100 μM. Values are the mean ± SD (n = 3). n.d.; not detected.

Donors / Acceptors	Trx (Yeast)	AsA	GSH	NADPH
	(nmol min^{-1} mg^{-1} protein)			
H_2O_2	127±10	831±21	157±6	n.d.
t-BOOH	117±15	131±22	92±26	n.d.
Cumene-OOH	68±13	88±17	72±35	n.d.

In trypanosomatids, peroxide detoxification has been shown to rely on a specific system consisting of the dithiol trypanothione (N^1,N^8-bis(glutathionyl) spermidine), flavoenzyme trypanothione reductase, and thioredoxin homologue tryparedoxin (Castro and Tomás, 2008). It is worth noting that trypanothione reductase has been reported previously in *Euglena* (Montrichard et al., 1999). Therefore, trypanothione/tryparedoxin system might contribute to regeneration of oxidized Prx as well as Trx/NTR system demonstrated in this study.

Effect of Prx suppression on cell growth

Euglena cells were previously shown to epigenetically suppress gene expression by the simple introduction of double-stranded RNA (dsRNA) into cells; however, the transformation procedure of *Euglena* has not yet been established (Iseki et al., 2002). Therefore, to evaluate the physiological significance of Prxs in *Euglena* cells, KD-*prx1 ~ 4* cells were generated by introducting dsRNA, synthesized from part of each *EgPrx* sequence, into *Euglena* cells using electroporation. The suppression of individual *Prx* gene expression levels in each KD-*prx* cell was confirmed by RT-PCR (**Figure II-6A**). KD-*prx2* and KD-*prx4* cells, in particular, exhibited the specific suppression of corresponding *Prx* gene expression. On the other hand, due to high sequence similarity of *Prx1* to *Prx3*, the expression of both *Prx3* and *Prx1* was more likely to be simultaneously suppressed in KD-*prx1* and KD-*prx3* cells, respectively. Considering the possibility that other *Prx* genes, except the targeted *Prx*, might compensate for the suppression effect, double KD-*prx* cells, including all EgPrx combinations, were generated by the simultaneous introduction of different dsRNAs. Although KD-*prx2/4* cells exhibited the specific suppression of *Prx* gene expression, the introduction of dsRNAs for individual *Prx1* and *Prx3* in other cells affected the expression of *Prx3* and *Prx1*, respectively, as well as single KD cells (**Figure II-6A**).

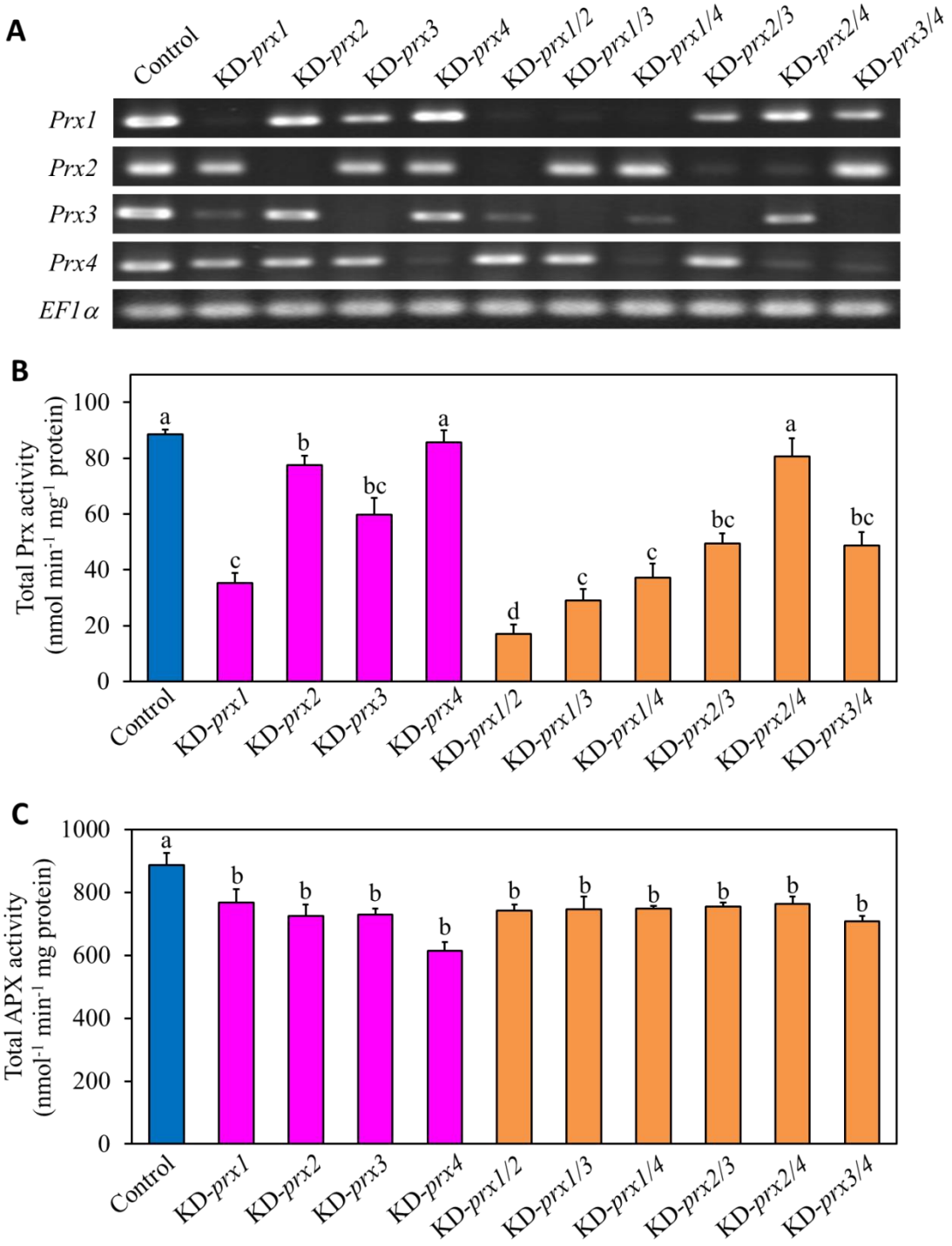
A
Control
KD-prx1
KD-prx2
KD-prx3
KD-prx4
KD-prx1/2
KD-prx1/3
KD-prx1/4
KD-prx2/3
KD-prx2/4
KD-prx3/4
Prx1
Prx2
Prx3
Prx4
EF1α
B
Total Prx activity
(nmol min-1 mg-1 protein)
0
20
40
60
80
100
a
c
b
bc
a
d
c
c
bc
a
bc
C
Total APX activity
(nmol-1 min-1 mg protein)
0
200
400
600
800
1000
a
b
b
b
b
b
b
b
b
b
b

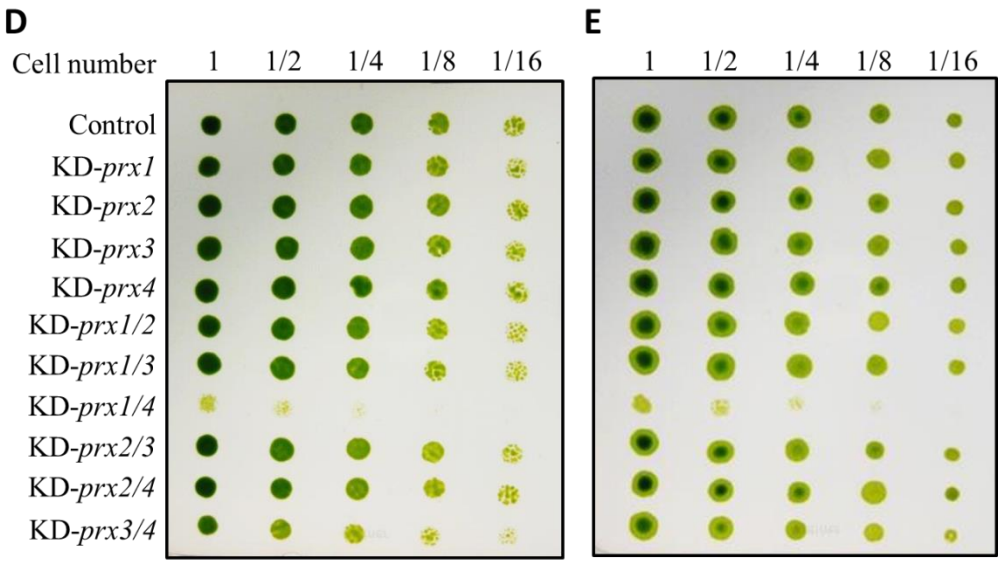

Figure II-6. Effect of Prx suppression on *Euglena* cells. (A) RT–PCR analysis of *Prx1~4* and *EF1α* (for normalization) mRNA levels using total RNA from *Euglena* cells in which dsRNA was introduced. The control represented cells electroporated without dsRNA. Fragments corresponding to *Prxs* and *EF1-α* were amplified by PCR using cDNA preparations as templates. (B and C) Prx and APX activities in extracts from each control and each KD cell, respectively. Values are the mean ± SD (n = 3). Values with different letters were significantly different according to the *t*-test ($p < 0.05$). (D and E) Cultures of control and each KD cell were spotted onto KH (heterotrophic) and CM (autotrophic) plates, respectively. The numbers of cells spotted were 4×10^4 (1), 2×10^4 (1/2), 1×10^4 (1/4), 5×10^3 (1/8), and 2.5×10^3 (1/16). Plates were incubated under normal conditions for 5 d.

Total Prx activity was significantly lower in all cells in which dsRNA was introduced, except KD-*prx4*, than in control cells that had been electroporated without dsRNA. KD-*prx1* cells exhibited the lowest Prx activity among the single KD cell lines, though the effect of co-suppression of other homologous *Prx* genes on total Prx activities is needed to consider. This result supports the high transcript levels of the *Prx1* gene, as shown in **Figure II-5**. In the case of double KD cell lines, total Prx

activities in KD-*prx1/2*, KD-*prx1/3* and KD-*prx1/4* cells were 19, 33 and 42% that of the control cells, respectively (**Figure II-6B**). As I predicted that Prx suppression would result in the upregulation of APX activity, followed by an ROS metabolism imbalance, total APX activities in control and KD-*prx* cells were also determined. APX activities in KD-*prx* cells ranged between 70 and 86% that of the control cells (**Figure II-6C**), suggested that the suppression of Prxs did not stimulate APX expression or post-transcriptional regulation.

To determine the effect of Prx suppression on cell growth, spot assays were performed using heterotrophic and autotrophic media. While the growth rates of all single KD-*prx*, KD-*prx1/2*, -*prx1/3*, -*prx2/3*, and -*prx2/4* cells were similar to that of the control cells, the growth rate of KD-*prx1/4* cells was markedly lower under normal heterotrophic and autotrophic growth conditions (**Figure II-6D, E**). The growth rate of KD-*prx3/4* cells was also decreased due to the high sequence similarity of *Prx1* to *Prx3*. These results suggest that the cytosolic 2-CysPrx and PrxII are essential for the normal growth of *Euglena* cells. Because of the lower gene expression of *EgPrx4* than that of *EgPrx1* (**Figure II-5**), EgPrx1, but not EgPrx4, was considered to function dominantly in the cytosol. However, the phenotypes of KD-*prx1/4* cells support the physiological importance of EgPrx4 in *Euglena*.

In *Schizosaccharomyces pombe*, peroxiredoxin Tpx1 regulates transcription factor Pap1, which in turn regulates antioxidant gene transcription in response to H_2O_2 (Vivancos et al., 2005). Fomenko et al. (2011) suggested that thiol peroxidases were the major regulators of global gene expression in response to H_2O_2 in *Saccharomyces cerevisiae*. Despite sufficient APX activity in KD-*prx1/4* cells, they showed several phenotypes (**Figure II-6C, D, E**). These results indicate that EgPrx1 and -4 are important not only for ROS scavenging, but also for redox signaling in the cytosol as well as in yeast thiol peroxidases.

In contrast to KD-*prx1/4* cells, the suppression of putative organelle-localized Prx (EgPrx2 and -3) did not induce a decrease in the cell growth rate. This may have occurred for the following reasons: (i) different unidentified thiol-peroxidases such as GPX may exist in chloroplasts and mitochondria; (ii) resistance of Calvin cycle enzymes to H_2O_2; and (iii) the diffusion of H_2O_2 generated in chloroplasts and mitochondria. In contrast to plants, photosynthesis in *Euglena* is not susceptible to

H_2O_2 due to the resistance of the fructose-1,6-/sedoheptulose-1,7-bisphosphatase, $NADP^+$-glyceraldehyde-3-phosphate dehydrogenase, and ribulose-5-phosphate kinase enzymes of the Calvin cycle to H_2O_2 up to 1 mM (Takeda et al., 1995). H_2O_2 generated in both chloroplasts and mitochondria in *Euglena* cells diffuses into the cytosol, where it is then subsequently decomposed by APX (Ishikawa et al., 1993).

2-CysPrxA and -B deficient *Arabidopsis* plants were shown to have significantly higher protein carbonylation and H_2O_2 levels. Protein carbonylation, in particular, was 4.7-fold higher in the mutant than in the wild type (Pulido et al., 2010). Nitrated protein levels were significantly higher in PrxIIE deficient *Arabidopsis* plants than in the wild type, while protein nitration was hardly detectable in PrxIIE overexpressing *Arabidopsis* plants, suggesting that PrxIIE detoxifies peroxynitrite in plants (Romero-Puertas et al., 2008). These findings support Prxs playing a critical role in defense against oxidative stress in plants. GPX5/GPXH-overexpressing *Chlamydomonas* cells showed increased tolerance to photooxidative stress (Ledford et al., 2007). In contrast to plant Prxs and *Chlamydomonas* GPX, the physiological significance of Prxs in almost all eukaryotic algae has not yet been evaluated. Our results on Prx KD cells will further understanding on the physiological functions of Prxs in eukaryotic algae.

Abstract

Euglena gracilis lacks catalase and contains ascorbate peroxidase (APX) which is localized exclusively in the cytosol. Other enzymes that scavenge reactive oxygen species (ROS) in *Euglena* have not yet been identified; therefore, ROS metabolism, especially in organelles, remains unclear in *Euglena*. The full-length cDNAs of four *Euglena peroxiredoxins* (*EgPrxs*) were isolated in this study. EgPrx1 and -4 were predicted to be localized in the cytosol, and EgPrx2 and -3 in plastids and mitochondria, respectively. The catalytic efficiencies of recombinant EgPrxs were similar to those of plant thiol-peroxidases, but were markedly lower than those of APX from *Euglena*. However, transcript levels of *EgPrx1*, *-2*, and *-3* were markedly higher than those of *APX*. The growth rate of *Euglena* cells, in which the expression of *EgPrx1* and *-4* was suppressed by gene silencing, was markedly reduced under normal conditions, indicating physiological significance of Prx proteins.

CHAPTER III

Biochemical and physiological analyses of NADPH-dependent thioredoxin reductase isozymes in *Euglena gracilis*

Introduction

Thioredoxins (Trxs) are small proteins (~12 kDa) that act as redox regulators in numerous cellular processes including metabolism, the synthesis of DNA, photosynthesis, respiration, and protein folding and repair (Arnér and Holmgren, 2000). Since Trxs are able to reduce thiol-containing peroxidases, peroxiredoxins (Prxs), they also play crucial roles in the metabolism of reactive oxygen species (ROS) as well as cellular redox regulation and other metabolic functions including the regulation of gene expression and molecular chaperone (Viera Dos Santos and Rey, 2006; Bhatt and Tripathi, 2011). The reducing power of Trxs is normally provided by NADPH in a reaction catalyzed by NADPH-dependent Trx reductase (NTR), which together form the so-called Trx system. NTR has been found in all types of organisms from bacteria to plants and animals. Two major classes of NTRs have been identified to date: (i) small type NTRs with a low molecular mass (~35 kDa), which are found in prokaryotes and some eukaryotes, and (ii) large type NTRs with a high molecular mass (~55 kDa) in some eukaryotes such as animals and protists (Jacquot et al., 2009). Photosynthetic organisms such as plants and algae have the enzyme NTRC, which is a bimodular enzyme formed by an NTR and Trx module in the same polypeptide (Serrato et al., 2004).

Among photosynthetic organisms, *Arabidopsis* NTRs have been characterized in detail. *Arabidopsis* NTRs are encoded by three genes and are distributed in three distinct cellular compartments: most NTRA are in the cytosol, most NTRB are in mitochondria, and NTRC exclusively exists in plastids (Serrato et al., 2004; Reichheld et al., 2005). The growth of an *Arabidopsis ntra ntrb* double knockout mutant was previously reported to be slower (Reichheld et al., 2007). The growth of an *Arabidopsis ntrc* knockout mutant was also found to be inhibited and it also exhibited hypersensitivity to different abiotic stresses, such as oxidative, drought, and salt stresses (Serrato et al., 2004). Genetic and biochemical analyses using an *Arabidopsis*

ntrc knockout mutant suggested that NTRC regulated the biosynthesis of starch and chlorophyll (Michalska et al., 2009; Richter et al., 2013). These findings indicate that NTRs are key regulators in various biological processes in plants. In contrast, although NTR genes have been identified in a few algal species such as *Chlorella vulgaris* and *Emiliania huxleyi* (Machida et al., 2009; Araie et al., 2008), their physiological significance in algae has not yet been established.

Euglena gracilis is a motile unicellular flagellate that can grow by photosynthesis and possesses an unusual cell membrane complex, the pellicle complex, but not a cell wall (Nakano et al., 1987). Metabolism in this organism was previously exhibited to be unique. For example, *Euglena* accumulates a large amount of paramylon (β-1,3 glucan) under aerobic conditions (Dwyer and Smillie, 1970). Under anaerobic conditions, *Euglena* synthesizes medium-chain wax esters from paramylon by a unique metabolic process called wax ester fermentation (Inui et al., 1982). We have been studying the molecular mechanisms underlying cellular redox regulation, including ROS metabolism, and their physiological roles in stress responses in *Euglena*. *Euglena* lacks catalase, but contains a single ascorbate peroxidase (APX), which is only localized in the cytosol. In contrast to APX in higher plants, the *Euglena* enzyme can reduce both H_2O_2 and alkyl hydroperoxides (Ishikawa et al., 2010). Furthermore, the activities of monodehydroascorbate, dehydroascorbate, and glutathione reductase have only been detected in the cytosol (Shigeoka et al., 1987a). These findings indicate the physiological significance of an ascorbate-dependent antioxidant system in the cytosol in *Euglena*. I recently identified four genes encoding Prx proteins in *Euglena*. *Euglena* Prxs were predicted to be localized in the cytosol, chloroplasts, and mitochondria. All enzymes exhibited the reduction activities of H_2O_2 and alkyl hydroperoxides. Knockdown (KD) experiments suggested that cytosolic Prx isoforms were essential for the normal growth of *Euglena* cells (Tamaki et al., 2014). These findings provided important evidence that the Trx-dependent antioxidant system is also a crucial regulator of cellular redox states in this alga. However, the roles of the Trx-dependent redox system(s) in ROS metabolism and other physiological processes remain largely unknown because Trx and NTR have not yet been identified in this organism.

I herein attempted to clarify Trx-dependent redox regulation in *Euglena* by searching for putative *NTR* genes. Three *NTR* genes were identified based on *Euglena* RNA-Seq data (Ishikawa et al., unpublished data), and named *EgNTR1*, *EgNTR2*, and *EgNTRC*. The enzymatic analysis of recombinant EgNTRs indicated that EgNTR2 had the highest catalytic efficiency, likely due to its molecular structure and catalytic mechanism of large type NTR. KD experiments suggested that EgNTR2 plays a key role in the homeostasis of cell growth and size in *Euglena* cells. To the best of our knowledge, this is the first study to have established the physiological importance of NTRs, especially in the cytosol, in eukaryotic microalga.

Materials and Methods

Strain and culture.

Euglena gracilis strain Z was grown in Koren-Hutner (KH) medium for heterotrophic growth (Koren and Hutner, 1967) or Cramer-Myers (CM) medium for autotrophic growth (Cramer and Myers, 1952) under continuous light conditions (50 μmol m^{-2} s^{-1}) at 26 ℃ with continuous shaking (120 rpm). Regarding the anaerobic treatment of the cells, the cultures were completely sealed and stood for 24 h after the replacement of air with nitrogen gas. Cell number and volume were determined using the electric field multi-channel cell counting system, CASY (Roche Diagnostics).

Construction of expression plasmids of recombinant Euglena NTRs.

Total RNA was isolated from *Euglena* cells, as previously described (Tamaki et al., 2014). First strand cDNA was synthesized using PrimeScript RT Master Mix (Takara) according to the manufacturer's instructions. The open reading frames of *Euglena* NTRs were amplified from first strand cDNAs using the following primer sets; EgNTR1-F (5'-GAGCTCATGTCCAAGCTGCTGC-3'), EgNTR1-R (5'-AAGCTTTCAGGGCTCGCCGT-3'), EgNTR2-F (5'-CATATGACGTCATACGACTATGACTACG-3'), EgNTR2-R (5'-AAGCTTTTAGCCGCACTTGC-3'), EgNTRCΔ-F (5'-GAGCTCCAATTGTTTTCGGG-3'), and EgNTRCΔ-R (5'AAGCTTCTAGTACTCGATGAGCAGC-3'). The amplified DNA fragments were

ligated into the pGEM-T easy vector (Promega) to confirm the absence of PCR errors. The resulting constructs were digested with Sac I and Hind III for EgNTR1 and EgNTRCΔ, and Nde I and Hind III for EgNTR2, and were ligated into the expression vector pCold II (Takara) to produce His-tagged proteins. The resulting plasmids were introduced into *Escherichia coli* strain BL21 Star cells (Agilent Technologies).

Expression and purification of recombinant proteins.

E. coli strain BL21 Star cells transformed with each pCold II/EgNTR were grown in 3 mL of LB medium containing 50 μg mL^{-1} of ampicillin. After an overnight culture at 37 °C, the cultures were transferred to 600 mL of LB medium (with the ampicillin) and grown to an A_{600} of 0.5. Isopropyl-1-thio-β-D-galactopyranoside (IPTG) was added to a concentration of 0.5 mM, and the cells were incubated for 20 h at 15 °C. All the buffers used for recombinant protein purification were prepared using metal ion-free water. The harvested cells were resuspended in 100 mM potassium phosphate buffer, pH 7.0, and were sonicated. His-tagged recombinant EgNTR proteins were purified using a TALON Metal Affinity resin (Clontech) according to the manufacturer's instructions. Protein contents were determined following the method of Bradford (Bradford, 1976). The purified enzymes were then desalted and concentrated using an ultrafiltration membrane (Amicon® Ultra-4; Millipore), and stored at −20 °C until later use.

Enzyme assay.

NTR activity was determined by the reduction of 5,5'-dithiobis(2-nitrobenzoic acid) (DTNB) according to the method described by Pascual et al. (2011). The reaction was performed in 100 mM potassium phosphate buffer, pH 7.0, 2 mM EDTA, 5 mM DTNB, 150 μM NADPH, and purified enzymes at the concentrations indicated in the table legends. The reduction of DTNB was monitored by increases in absorbance at 412 nm.

RNA interference (RNAi) experiments.

The KD of EgNTRs by RNAi was performed as described previously (Tamaki et al., 2014). Approximately 500-bp partial cDNA templates of EgNTRs with the T7

RNA polymerase promoter (underlined in the primer sequences below) were amplified using the following primer sets EgNTR1/RNAi-F (TAATACGACTCACTATAGGGGCTTTTCCAAGGGCATC), EgNTR1/RNAi-R (TAATACGACTCACTATAGGGTCACCTTCACACCGGTC), EgNTR2/RNAi-F (TAATACGACTCACTATAGGGAAGAAGCTGATGCACTACGC), EgNTR2/RNAi-R (TAATACGACTCACTATAGGGTTCTCGGAGCACTGGC), EgNTRC/RNAi-F (TAATACGACTCACTATAGGGTACAACACAGCGGTGGAAG), and EgNTRC/RNAi-R (TAATACGACTCACTATAGGGCGACTCGTGGTACAGTTTC). Double-stranded RNA (dsRNA) was synthesized from PCR products as templates using the MEGAscript RNAi Kit (Life Technologies) according to the manufacturer's instructions. *Euglena* cells from seven-day-old cultures grown in CM medium were harvested and resuspended in CM medium. *Euglena* cells grown in KH medium for two days were used for heterotrophic conditions. Approximately 15 μg of dsRNA was introduced into the cell suspension (100 μL; approximately 5×10^6 cells) using the NEPA21 electroporator (Nepa Gene). The cell suspension was inoculated into fresh medium and cultured at 26 °C for restoration.

RT-PCR analysis.

Total RNAs were isolated from 2-week-old *Euglena* cells into which dsRNA were introduced. Gene silencing was then confirmed by RT-PCR using RNAi primer sets as described above. EgEFα was chosen as a control using the following primers; EgEF1α-F (5'-GCCTCTTCGCCTCCCACTG-3'), and EgEF1α-R (5'-TTCATCAGGACAATCGCAGCA-3'). PCR amplification was performed with 22–34 cycles of 95 °C for 30s, 58 °C for 30s, and 72 °C for 40s. The PCR products were analyzed on 1% agarose gels. Equal loading of each amplified gene sequence was determined with the control EgEF1α PCR product.

Microscopy analysis.

Cells cultured for 32 days after the introduction of dsRNA were observed. Images were recorded using an Olympus BX51 upright microscope through a 40× objective lens (Olympus).

Paramylon determination.

Paramylon was extracted from *Euglena* cells according to the method described by Sugiyama et al. (2010). *Euglena* cells harvested by centrifugation were freeze-dried. After being suspended in acetone, the cells were sonicated and paramylon was harvested. To remove lipids and proteins, this rough paramylon was treated at 100 °C for 30 min with 1% SDS solution. Paramylon was obtained after further centrifugation, and, following repeated washing with 0.1% SDS solution and H_2O, refined paramylon was obtained. Paramylon was solubilized with 0.5 N NaOH and determined by the phenol-sulfuric acid method.

Wax ester determination.

The extraction of the total wax ester fraction from *Euglena* cells was performed according to the method described by Inui et al. (1982). *Euglena* cells were harvested, freeze-dried, and added to 2.4 mL of a mixture of chloroform, methanol, and water in the ratio 10:20:8 (v/v/v). After thorough agitation, the mixture was centrifuged to remove cells and debris. The extraction was repeated, and the combined supernatants were added to 1 ml each of chloroform and water, followed by vigorous shaking. After centrifugation, the chloroform phase was evaporated and dissolved in hexane. The wax ester extract was filtrated using the PTFE 0.22 μm filter for the gas chromatography-mass spectrometry (GC-MS) analysis. The wax ester fraction was separated and determined using GCMS-QP2010 (Shimadzu). Separation was performed on an Agilent J&W DB-5ms column (30 m × 0.25 mm internal diameter, 0.25 μm film thickness; Agilent Technologies). A 1-μL portion of the wax ester fraction was injected into GC-MS using a splitless injection; helium was used as the carrier gas (1.16 mL/min). Chromatographic separation was initially set at 100 °C (1 min), then the temperature was increased to 280 °C (10 °C per min), and held for 10 min. The mass transfer line and ion source were at 250 °C. Myristyl myristate was detected with electron ionization (70 eV) in the selected ion monitoring mode at m/z 229.2 and 57.1 for the quantitative analysis.

Results and Discussion

Identification of NTR genes in Euglena

Three *NTR* genes of *Euglena* were identified by homology search in *Euglena* RNA-Seq data (Ishikawa et al., unpublished data). The cDNA sequence of each *EgNTR* gene had a unique spliced leader sequence, which was a common short sequence usually found at the 5' end of *Euglena* transcripts (Tessier et al., 1991), indicating that these cDNA sequences were full-length cDNAs.

NTRs are generally classified into three representative subclasses such as small and large types and NTRC as described in introduction. Thus, based on the known classification, the three cDNAs were named *EgNTR1*, *EgNTR2,* and *EgNTRC* (accession numbers AB853316, AB853317, and AB853318, respectively). Sequence comparisons of EgNTRC with known NTRCs revealed that EgNTRC was a bimodular enzyme formed by an NTR module and Trx module (Serrato et al., 2004). As shown in **Table III-1**, although no Trx module was found in EgNTR1, it showed significant identity (54%) with EgNTRC. Since the NTR module of NTRC typically belongs to the small type, it was suggested that EgNTR1 was classified as the small type. This was also supported by EgNTR1 and EgNTRC both being highly identical (53~62%) to known small type NTRs and NTRCs. In contrast, EgNTR2 had 50~59% identity with large type NTRs, but low identity (15~25%) with small type NTRs and NTRCs. Thus, it was suggested that EgNTR2 was classified as the large type.

Table III-1. Amino acid sequence identities between NTRs from *Euglena* and other organisms. The percentage identities of *Euglena* NTRs to each other and with NTRs from other organisms were calculated.

Organism	Enzyme	Subclass	Identity (%)		
			EgNTR1	EgNTR2	EgNTRC
Euglena gracilis	NTR1	Small		29	54
	NTR2	Large	29		21
	NTRC	NTRC	54	21	
Homo sapiens	NTR1	Large	22	50	30
	NTR2	Large	26	51	21
Plasmodium falciparum	NTR	Large	26	59	20
Plasmodium vivax	NTR	Large	24	58	24
Saccharomyces cerevisiae	NTR1	Small	60	25	56
	NTR2	Small	56	22	54
Arabidopsis thaliana	NTRA	Small	56	33	53
	NTRB	Small	57	25	53
	NTRC	NTRC	58	15	62
Chlamydomonas reinhardtii	NTR1	Large	23	53	20
	NTR3	Small	54	17	54
	NTRC	NTRC	58	17	60
Chlorella vulgaris	NTRC	NTRC	56	18	62

The sequence alignments of *Euglena* NTRs with the known NTRs were shown in **Figure III-1**. EgNTR1 and EgNTRC included the conserved Cys residues (Cys142 and -145 in EgNTR1, and Cys327 and -330 in EgNTRC) in the active site. These sequences also had the sites for binding NADPH and FAD (Wulff et al., 2011). Moreover, EgNTRC contained the conserved Cys residues (Cys570 and -573) in the Trx module active site. EgNTR2 had the conserved Cys residues (Cys52 and -57) in the active site, found in known large type NTRs (Arnér and Holmgren, 2000). Among the large type NTRs, NTRs from mammals and eukaryotic algae have been shown to have a Se-Cys at the C-terminus, but not in malaria parasites (Snider et al., 2014). The

C-terminal sequence of EgNTR2 lacked a Se-Cys, which corresponded to that of the parasites (*Plasmodium falciparum* and *P. vivax*). The phylogenetic tree showed that EgNTR1, EgNTR2, and EgNTRC were close to small, large, and NTRC type clades, respectively (**Figure III-2**). EgNTR2, in particular, was very close to NTRs from malaria parasites, but not from eukaryotic algae. Thus, the phylogenetic analysis suggested that NTRs from *Euglena* and the apicomplexa phylum including malaria parasites shared a common ancestor.

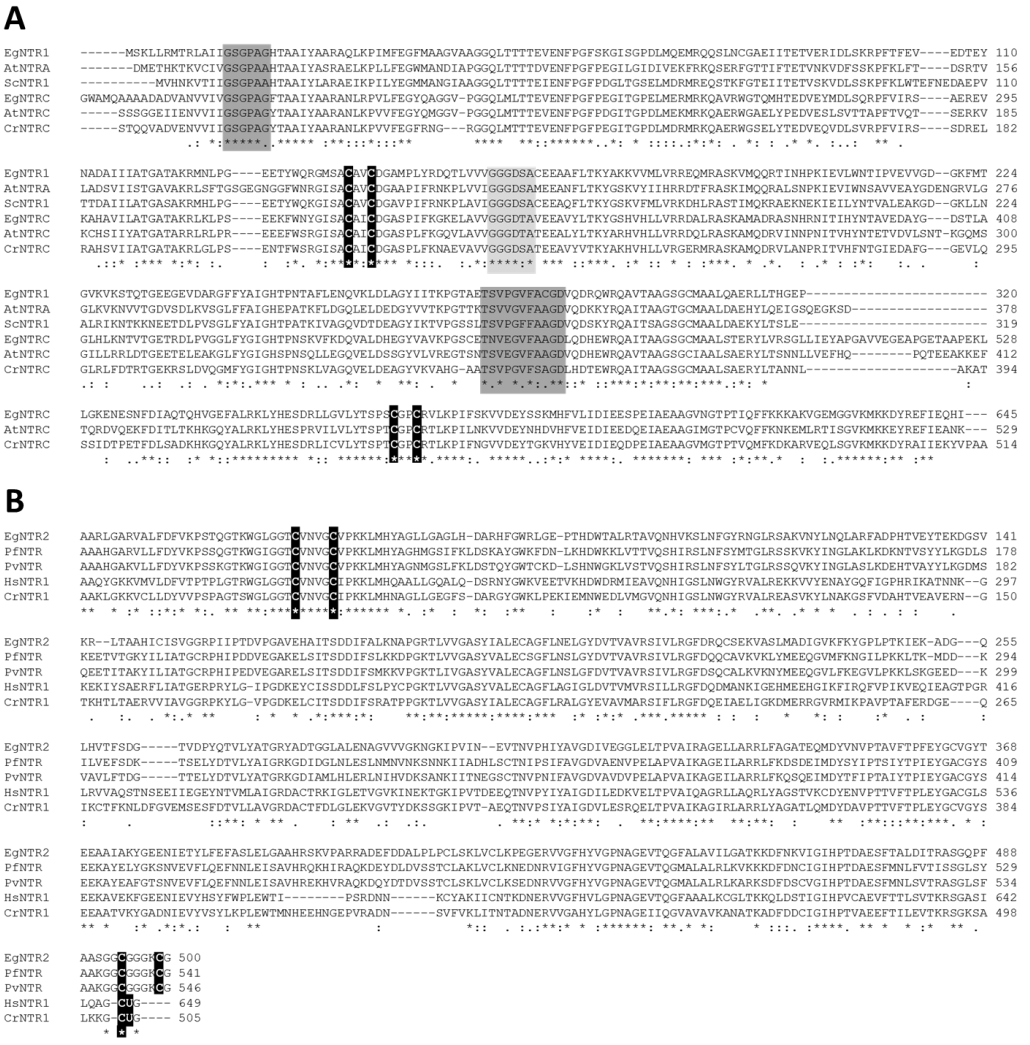

Figure III-1. Sequence alignments of *Euglena* NTR proteins with known NTRs. Partial sequence alignments of (A) EgNTR1 and EgNTRC with small type NTRs from *Arabidopsis thaliana* (AtNTRA, Q39242; AtNTRC, O22229), *Saccharomyces cerevisiae* (ScNTR1, P29509), and *Chlamydomonas reinhardtii* (CrNTRC, A8HNQ7) and (B) EgNTR2 with large type NTRs from *Plasmodium falciparum* (PfNTR, Q25861), P. vivax (PvNTR, A5K6V2), *Homo sapiens* (HsNTR1, B2R5P6), and *C. reinhardtii* (CrNTR1, A8J448). Letters shown in white on a black background represent conserved Cys and Se-Cys residues in the active site. FAD and NADPH binding sites are highlighted in dark gray and light gray, respectively. Asterisks indicate the amino acids conserved in all sequences, and colons and dots indicate amino acids with similar biochemical characteristics.

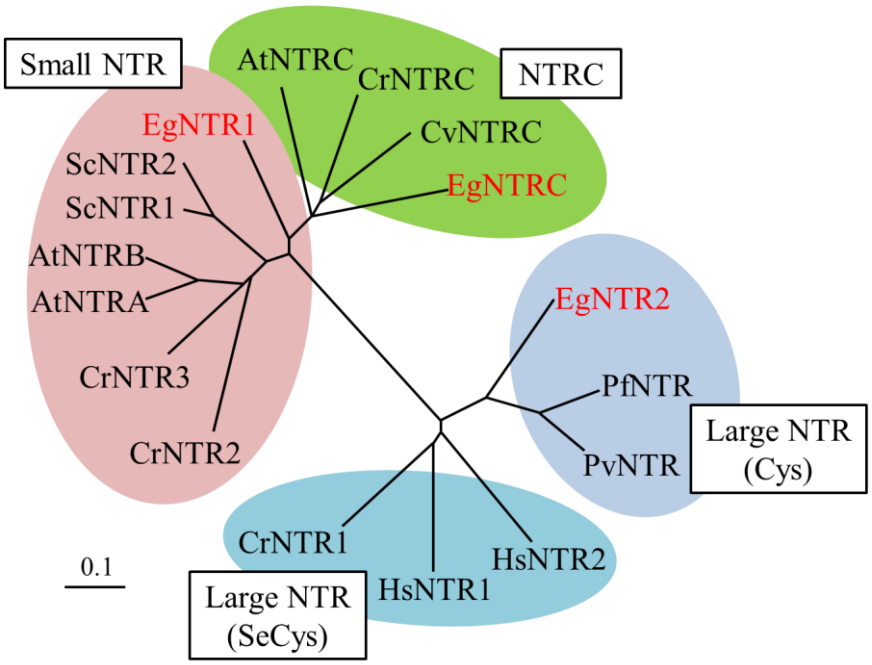

Figure III-2. Phylogenetic relationship between NTRs from *Euglena* and other organisms. The phylogenetic tree was constructed with full-length NTR amino acid sequences using the ClustalW program. Large type NTRs were divided into clades with or without Se-Cys at their C-terminal region. Abbreviations and UniProt accession numbers for the NTR orthologues are as follows: At, *A. thaliana* (AtNTRA, Q39242; AtNTRB, Q39243; AtNTRC, O22229); Cr, *C. reinhardtii* (CrNTR1, A8J448; CrNTR2, A8I208; CrNTR3, A8JFV6; CrNTRC, A8HNQ7); Cv, *Chlorella vulgaris* (CvNTRC, B9ZYY5); Sc, *S. cerevisiae* (ScNTR1, P29509; ScNTR2, P38816); Hs, *H. sapiens* (HsNTR1, B2R5P6; HsNTR2, Q9NNW7); Pf, *P. falciparum* (PfNTR, Q25861); Pv, *P. vivax* (PvNTR, A5K6V2).

Predictions of the existence of transit peptides in the deduced amino acid sequences of *Euglena* NTRs were performed using the TMHMM (http://www.cbs.dtu.dk/services/TMHMM/) and TargetP (http://www.cbs.dtu.dk/services/TargetP/) programs. The TMHMM program showed that EgNTRC had three transmembrane domains at the N-terminal region (**Figure III-3C**). Since *Euglena* is a secondary symbiont, its chloroplasts are surrounded by three layer envelopes, unlike chloroplasts from plants. Thus, the plastid-targeting signal is completely different from that in plants, and, as for the signal, two transmembrane helices were shown to exist at the N-terminal region of plastid-targeted proteins (Durnford and Gray, 2006). In agreement with the localization of NTRCs from plants, it was suggested that EgNTRC was localized in plastids. The TargetP program is not suitable for predicting plastid-targeting signals in *Euglena*. The third transmembrane domain of EgNTRC, which contains a conserved FAD binding site, is likely irrespective of import into plastids. The TargetP program predicted that EgNTR1 was localized in mitochondria (**Figure III-3D**). In most cases, *Euglena* mitochondria-targeted proteins contain an arginine-rich motif within hydrophobic amino acids at the N-terminus (Krnáčová et al., 2012). Since 10 N-terminal amino acids of EgNTR1 are rich in arginine, methionine, and leucine (**Figure III-3E**), EgNTR1 appeared to be localized in mitochondria. The existence of a characteristic organelle-targeting peptide in EgNTR2 was not predicted by either program, suggested the localization of EgNTR2 in the cytosol. The calculated molecular masses of the full-length forms of EgNTR1 and EgNTR2, and predicted mature EgNTRC were 34.6, 53.2, and 51.8 kDa, respectively.

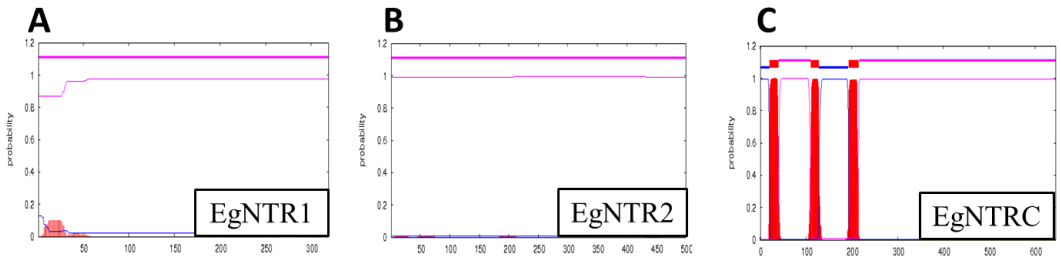

D

Name	Len	cTP	mTP	SP	other	Loc
EgNTR1	319	0.009	0.894	0.060	0.161	M
EgNTR2	500	0.049	0.243	0.225	0.824	—
EgNTRC	645	0.103	0.462	0.006	0.587	—

E

```
                1         10
EgNTR1          MSKLLRMTRL
```

Figure III-3. Prediction of transmembrane domains and subcellular localization of *Euglena* NTRs. (A-C) Predicted transmembrane domains of *Euglena* NTRs using the TMHMM program. (D) Predicted localization of *Euglena* NTRs using the TargetP program. Values represent the possibility of the chloroplast transit peptide (cTP), mitochondrial-targeting peptide (mTP), and secretory pathway signal peptide (SP). Loc, predicted localization; M, mitochondria. (E) 10 N-terminal amino acids of EgNTR1. Bold letters are arginine and hydrophobic (methionine and leucine) residues.

Enzymatic characterization of recombinant Euglena NTRs

To examine the enzymatic properties of EgNTRs, each recombinant EgNTR protein was expressed in *E. coli* and purified to apparent homogeneity, as judged by SDS-PAGE (**Figure III-4**). While EgNTR1 appeared to have a putative very short mitochondria-targeting signal-like peptide, recombinant EgNTR1 was expressed as a full-length form. Recombinant EgNTRC was expressed as a truncated form without both the plastid-targeting peptide and Trx domain, and was named EgNTRCΔ. NTR activity was assayed by the reduction of DTNB. All recombinant EgNTRs showed significant DTNB reduction activities. To test the electron donor specificity of

recombinant EgNTRs, enzyme activities were measured using NADPH and NADH as electron donors. Using NADPH, the specific activities of EgNTR1, EgNTR2, and EgNTRCΔ were 0.92, 7.32, and 0.55 μmol min^{-1} mg^{-1} protein, respectively (**Table III-2**). By contrast, the specific activities of EgNTR1 and EgNTR2 using NADH were markedly lower, or not detectable, and the specific activity of EgNTRCΔ was 36% using NADPH. These results suggested that electron donor affinities differed between EgNTRC and other EgNTRs.

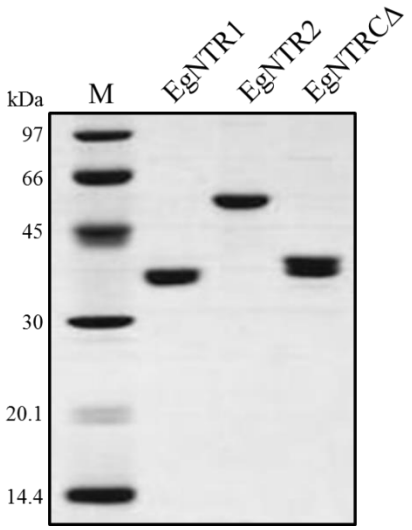

Figure III-4. SDS-PAGE of purified recombinant *Euglena* NTRs. *E. coli* cells harboring the pCold II construct were incubated with 0.5 mM IPTG for 20 h at 15 °C. Each recombinant enzyme purified using a TALON® Metal Affinity Resin was analyzed by 12.5% SDS-PAGE.

Table III-2. Electron donor specificity of recombinant *Euglena* NTRs. NTR activities toward DTNB were measured using 150 μM NADPH or NADH as the electron donor. Values are the mean ± SD (n=3). n.d.; not detectable.

Enzyme	NADPH	NADH
	(μmol min^{-1} mg^{-1} protein)	
EgNTR1	0.92±0.03	0.02±0.01
EgNTR2	7.32±0.11	n.d.
EgNTRCΔ	0.55±0.02	0.20±0.02

The kinetic properties of recombinant EgNTRs were examined. As shown in **Table III-3**, the V_{max}, K_m, and k_{cat} values of EgNTR2 for NADPH were determined to be 7.02 μmol min^{-1} mg^{-1} protein, 5.6 μM, and 383 min^{-1}, respectively. The K_m and k_{cat} values of EgNTR2 for DTNB were determined to be 2.5 mM, and 642 min^{-1}, respectively. These kinetic properties were similar to those of *P. falciparum* NTR (Gilberger et al., 1997; Müller et al., 1996) in consistent with their molecular structures. The K_m and k_{cat} values of EgNTR1 for NADPH were determined to be 22.4 μM, and 35.5 min^{-1}, while those of EgNTRCΔ were 24.7 μM, and 58.0 min^{-1}, respectively, indicating the similar kinetic parameters of both enzymes for NADPH. On the other hand, the K_m value of EgNTRCΔ for NADH was determined to be 80.6 μM. Considering the fact that the K_m values of wheat NTR and rice NTRC for NADH were 0.6 mM, and 1.2 mM, respectively (Serrato et al., 2004; Serrato et al., 2002), EgNTRC appeared to have higher affinity for NADH than NTRs from plants. However, the catalytic efficiencies (k_{cat}/K_m) of EgNTRCΔ for NADPH and NADH were determined to be 3.95×10^4 and 2.48×10^3 M^{-1} sec^{-1}, respectively; therefore, the physiologically dominant electron donor of EgNTRC appeared to be NADPH. Although EgNTR1 was predicted to be localized in mitochondria, this preferably used NADPH over NADH at least *in vitro*. This property was similar to that of *Arabidopsis* mitochondrial AtNTRB (Laloi et al., 2001). The K_m and k_{cat} values of EgNTR1 for DTNB were determined to be 2.4 mM and 52.9 min^{-1}, respectively, while those of EgNTRCΔ were 11.9 mM and

73.5 min^{-1}, respectively. The K_m value of EgNTRCΔ was approximately 5-fold higher than that of EgNTR1, and this might be attributed to deletion of the Trx module in EgNTRC. The catalytic efficiency of EgNTR2 (1.22×10^6 M^{-1} sec^{-1}) for NADPH was 30~46-fold higher than those of EgNTR1 and EgNTRCΔ ($2.65\sim3.95 \times 10^4$ M^{-1} sec^{-1}), and may have been caused by structural and catalytic differences between EgNTR2 and other EgNTRs. Together, our findings demonstrated that all EgNTRs can act as NTRs, and the large type EgNTR2 can reduce DTNB more efficiently than the small type NTRs, EgNTR1 and EgNTRC. Since most species, except for eukaryotic algae, contain either small or large type NTRs, the enzymatic characterization of EgNTRs will provide important insights into the molecular evolution of NTRs.

Table III-3. Kinetic parameters of recombinant *Euglena* NTRs. NAD(P)H and DTNB were used at a concentration in the range of 2.5-150 μM and 0.5-20 mM, respectively. Recombinant EgNTR1 and EgNTRCΔ were added at a concentration of 0.4 μM, and EgNTR2 at 0.02 μM. Values are the mean ± SD (n=3).

Enzyme	Substrate	V_{max} (μmol min^{-1} mg^{-1})	K_m (μM)	k_{cat} (min^{-1})	k_{cat} / K_m (M^{-1} sec^{-1})
EgNTR1	NADPH	0.98±0.06	22.4±2.1	35.5±2.3	2.65×10^4
EgNTR2	NADPH	7.02±1.35	5.6±2.2	383±74	1.22×10^6
EgNTRCΔ	NADPH	1.50±0.09	24.7±3.4	58.0±3.4	3.95×10^4
	NADH	0.31±0.03	80.6±8.9	11.9±1.0	2.48×10^3
Enzyme	Substrate	V_{max} (μmol min^{-1} mg^{-1})	K_m (mM)	k_{cat} (min^{-1})	k_{cat} / K_m (M^{-1} sec^{-1})
EgNTR1	DTNB	1.45±0.22	2.4±0.5	52.9±7.9	3.77×10^2
EgNTR2	DTNB	11.8±0.9	2.5±0.3	642±50	4.33×10^3
EgNTRCΔ	DTNB	1.90±0.20	11.9±1.7	73.5±7.7	1.03×10^2

Physiological role of Euglena NTRs

To examine the physiological role of *Euglena* NTRs, KD cell lines (KD-*ntr1*, -*ntr2*, and -*ntrc*) were generated by electroporational dsRNA transfer into *Euglena* cells grown autotrophically. The suppression of individual *EgNTR* gene expression in each KD-*ntr* cell was confirmed by an RT-PCR analysis. As shown in **Figure III-5A**, corresponding gene expression in all KD-*ntr* cells was specifically suppressed. The growth rate of KD-*ntrc* cells was similar to control cells, while those of KD-*ntr1* and -*ntr2* cells were significantly lower than that of control cells (**Figure III-5B**). The growth of KD-*ntr2* cells stopped approximately 12 days after the introduction of dsRNA.

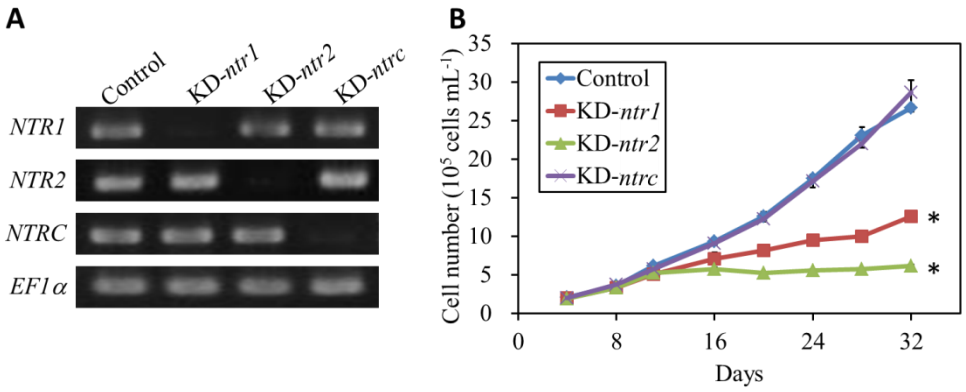

Figure III-5. Effects of EgNTR suppression on cell growth. (A) Transcript levels of *EgNTR1*, *EgNTR2*, *EgNTRC*, and *EgEF1α* (P14963; for constitutive control) in the control and each KD-*ntr* cell. The control represented cells electroporated without dsRNA. A RT-PCR analysis was performed using specific primers for *EgNTR1*, *EgNTR2*, *EgNTRC*, and *EgEF1α* with cDNA preparations from the control and each KD cell. (B) Growth rates of the control and each KD cell. Cells were grown autotrophically under continuous light (50 μmol m^{-2} s^{-1}) at 26°C for 32 days. Values are the mean ± SD (n = 3). Values with asterisks were significantly different, according to the *t*-test ($p < 0.05$).

Although NTRC is responsible for various chloroplastic processes including defense against oxidative stress (Cejudo et al., 2012), growth rates were not affected by the suppression of *EgNTRC* expression in *Euglena* cells. This result suggests a functional compensation by other reductase(s). Ferredoxin-dependent Trx reductase (FTR) is found in photosynthetic organisms, and functions as a chloroplastic Trx reductase during the light period when reduced ferredoxin is available (Schürmann and Buchanan, 2008). A putative *FTR* gene existed in our *Euglena* RNA-Seq data (data not shown). Therefore, the FTR gene may mimic NTRC functions in KD-*ntrc* cells.

The cell volume of KD-*ntr2* cells was unexpectedly 3.4-fold higher than that of control cells for 32 days after the introduction of dsRNA. The cell volume of KD-*ntr1* cells also increased slightly, while that of KD-*ntrc* cells was similar to that of control cells (**Figure III-6**). These results suggested that EgNTRs, especially EgNTR2, play a key role in the homeostasis of cell growth and size in *Euglena* cells. To understand whether the redox perturbation in the cytosol leads to cell hypertrophy in more detail, I checked the cell volume of *Euglena* cell lines with reduced expression of *APX*, *Prx1*, and *Prx4*, which act as cytosolic peroxidases (Ishikawa et al., 2010; Tamaki et al., 2014). The results obtained showed that cell volumes in KD-*apx* and -*prx1/4* cells remained unchanged (data not shown). Thus, it is likely that EgNTRs regulate cell size irrespective to ROS levels in the cytosol. In eukaryotic cells, Trx system also regulates a key enzyme of DNA synthesis, ribonucleotide reductase, by dithiol/disulfide exchange reaction (Holmgren and Sengupta, 2010). Thus, cell hypertrophy in KD-*ntr2* cells may be due to inhibition of DNA synthesis. Further analysis will be necessary to explain the molecular mechanism underlying phenomenon in KD-*ntr2* cells.

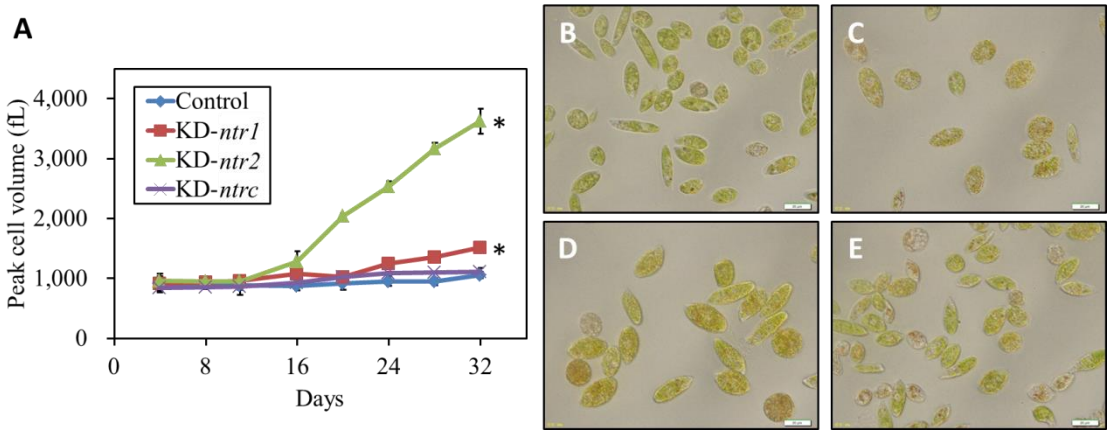

Figure III-6. Effects of EgNTR suppression on cell morphology. (A) Cell volumes of the control and each KD-*ntr* cell. Values are the mean ± SD (n = 3). Values with asterisks were significantly different, according to the *t*-test ($p < 0.05$). (B-E) Photographs of (B) control, (C) KD-*ntr1*, (D) KD-*ntr2*, and (E) KD-*ntrc* cells. Photographs showed cells cultured for 32 days. Scale bars are 20 μm.

Euglena converts paramylon, a storage β-1,3 glucan, into medium-chain wax esters after switching from aerobic to anaerobic conditions. This metabolic process is referred to as wax ester fermentation because of the simultaneous net synthesis of ATP (Inui et al., 1982). Since oxygen sensing is one of the key factors for wax ester fermentation, the relationship between wax ester fermentation and redox regulation was also examined. As the results, the contents of paramylon and myristyl myristate (C14:0-C14:0) in heterotrophically grown KD-*ntr* cells were similar to those in control cells under both aerobic and anaerobic conditions (**Figure III-7**), strongly suggesting that Trx systems did not contribute to the control of wax ester fermentation.

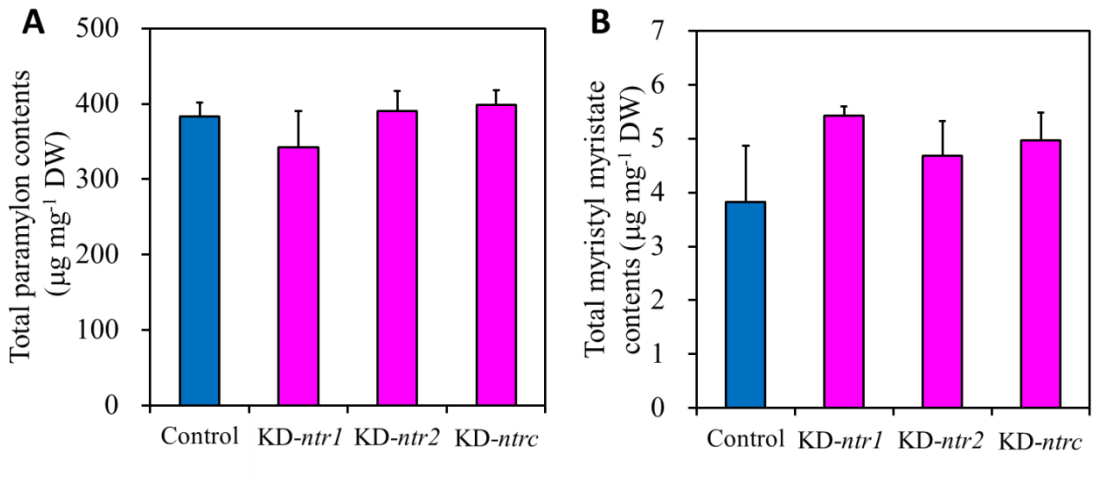

Figure III-7. Effects of EgNTR suppression on wax ester fermentation. (A) Total paramylon contents of the control and each KD-*ntr* cell. Aerobically grown cells were harvested. (B) Total myristyl myristate contents of the control and each KD cell. Aerobically grown cells were transferred to anaerobic conditions for 24 h and then harvested. Values are the mean ± SD (n = 3).

In conclusion, I identified three genes encoding NTR enzymes in *Euglena*, and characterized these enzymes. Unlike the well-characterized NTRs from animals and plants, *Euglena* exhibited the phylogenetic diversity of NTRs. An enzymatic analysis indicated that all EgNTRs were biologically functional enzymes, and EgNTR2, which belongs to large type NTRs, had the highest catalytic efficiency of the three EgNTRs. Silencing experiments showed that the suppression of *EgNTR2* gene expression affected growth rates and cell volumes, suggesting that EgNTR2 plays a key role in the homeostasis of cell growth and size in *Euglena* cells.

ROS metabolism in trypanosomatids, which belong to the protist phylum Euglenozoa as well as *Euglena*, depends on an alternative redox system consisting of tryparedoxin, trypanothione (N^1,N^8-bis(glutathionyl) spermidine), and trypanothione reductase, but not a Trx system (Castro and Tomás, 2008). Trypanothione has been detected in some parasites, except for trypanosomatids (Ondarza et al., 1999; Ondarza

et al., 2006). It is worth mentioning that a previous study demonstrated the existence of trypanothione reductase in *Euglena* (Montrichard et al., 1999). A putative trypanothione reductase gene, the deduced amino acid sequence of which contains the reported peptide sequence (KMGATIRDFYTTIGVH), was identified in our *Euglena* RNA-Seq data (data not shown). *Euglena* is a fascinating model for research on the evolution of both Trx- and trypanthione-dependent pathways. Furthermore, this study revealed that *Euglena* had NTRC type enzyme found in only photosynthetic organisms, suggesting the dual aspects of *Euglena* thiol redox systems as photosynthetic organism and protist. Therefore, further analysis needs to fully understand the significance to earn different photosynthetic organism and protists-specific thiol redox systems in *E. gracilis*.

Abstract

At least four peroxiredoxins that are coupled with the thioredoxin (Trx) system have been shown to play a key role in redox metabolism in the unicellular phytoflagellate *Euglena gracilis*. In order to clarify Trx-mediated redox regulation in this alga, I herein identified three NADPH-dependent thioredoxin reductases (NTRs) using a homologous search and characterized their enzymatic properties and physiological roles. Each *Euglena* NTR protein belonged to the small, large, and NTRC types, and were named EgNTR1, EgNTR2, and EgNTRC, respectively. EgNTR2 was phylogenetically different from the known NTRs in eukaryotic algae. EgNTR1 was predicted to be localized in mitochondria, EgNTR2 in the cytosol, and EgNTRC in plastids. The catalytic efficiency of EgNTR2 for NADPH was 30~46-fold higher than those of EgNTR1 and truncated form of EgNTRC, suggested that large type EgNTR2 reduced Trx more efficiently. The silencing of *EgNTR2* gene expression resulted in significant growth inhibition and cell hypertrophy in *Euglena* cells. These results suggest that EgNTRs function in each cellular compartment and are physiologically important, particularly in the cytosol.

CHAPTER IV

Comparative and functional analyses of glutathione reductase and trypanothione reductase in *Euglena graclis*

Introduction

Glutathione (GSH) is a low-molecular-weight thiol tripeptide, constituted by glutamate (Glu), cysteine (Cys), and glycine (Gly), in all organisms. GSH is synthesized in two steps catalyzed by γ-glutamylcysteine synthetase (GSH1) and glutathione synthetase (GSH2) (Noctor et al., 2002). GSH is continuously oxidized to a disulphide form (GSSG) that is recycled to GSH by NADPH-dependent glutathione reductase (GR). The GSH/GR system is involved in reactive oxygen species (ROS) metabolism as a component of ascorbate (AsA)-GSH cycle, consisting of ascorbate peroxidase (APX), monodehydroascorbate reductase (MDAR), dehydroascorbate reductase (DHAR), and GR (Noctor and Foyer, 1998). GR belongs to a member of the FAD-binding disulfide oxidoreductase superfamily. Among photosynthetic organisms, *Arabidopsis* GRs have been characterized in detail. *Arabidopsis* GRs are encoded by two genes, and GR1 is found in the cytosol and peroxisome, while GR2 in chloroplast and mitochondria (Chew et al., 2003; Kataya and Reumann, 2010). *Arabidopsis gr2* knockout mutant was embryo lethal (Tzafrir et al., 2004), while mutant deficient in GR1 and major leaf catalase CAT2 accumulated GSSG massively. The *gr1* mutation in *Arabidopsis* affected responses to pathogens and gene expression involved in hormone signalling (Mhamdi et al., 2010). These findings indicate the physiological significance of GSH/GR system as a cellular redox regulator. Recently, gene encoding GR in *Chlamydomonas* sp. ICE-L have been identified (Ding et al., 2012), while their physiological role in algae is poorly understood.

On the other hand, protozoan parasites trypanosomatids such as *Trypanosoma cruzi* and *Leishmania major* lack GR (Fairlamb et al., 1985), and many of the functions based on GSH/GR system is replaced by N^1,N^8-bis(glutathionyl)spermidine (trypanothione, $T(SH)_2$) and trypanothione reductase (TRYR) (Fairlamb and Cerami, 1992). $T(SH)_2$ is synthesized by the ATP-dependent stepwise conjugation of two GSH and one spermidine molecules (Comini et al., 2003; Oza et al., 2005). $T(SH)_2$

participates in numerous physiological pathways, especially plays an essential role in ROS metabolism. Trypanosomatids contain three distinct peroxidases: peroxiredoxin (Prx), glutathione peroxidase (GPX)-like enzyme, and APX (Castro and Tomás, 2008). Prx and GPX-like enzyme use tryparedoxin, thioredoxin (Trx)-related protein with the atypical active site, and APX uses AsA as electron donors, and regeneration of them depends on $T(SH)_2$. Oxidized form of trypanothione (TS_2) is recycled back to reduced form by the TRYR at the expense of NADPH. TRYR also belongs to the family of FAD-binding disulfide oxidoreductases, and shares many physical and chemical properties with GR. As supported its physiological importance, TRYR have been shown to be critical for survival and/or infectivity in *L. donovani* and *T. brucei* (Müller et al., 2003).

Euglena gracilis is a unicellular phytoflagellate, which belongs to the protist phylum Euglenozoa as well as trypanosomatids. As ROS metabolism in eukaryotic algae has not yet been established, we have been studying molecular mechanisms of ROS metabolism in *Euglena*. *Euglena* lacks catalase, but contains a single APX, which localized exclusively in the cytosol. Unlike APXs in plants and trypanosomatids (Shigeoka et al., 2002; Wilkinson et al., 2002), *Euglena* APX can reduce both of H_2O_2 and alkyl hydroperoxides. Silencing experiments indicated physiological importance of APX in the metabolism of cellular H_2O_2 levels in *Euglena* cells (Ishikawa et al., 2010). Enzymatic activities of MDAR, DHAR, and GR of the AsA-GSH cycle, have been also located exclusively in the cytosol (Shigeoka et al., 1987a). I recently identified four genes encoding Prx enzymes in *Euglena*, and they displayed the reduction activities of both H_2O_2 and alkyl hydroperoxides as well as plant Prxs. In addition, three genes encoding NADPH-dependent Trx reductases (NTRs), which are responsible for the regeneration of Prx, also identified. *Euglena* Prxs and NTRs were predicted to localize in the cytosol, chloroplasts, and mitochondria, indicated the existence of organelle-specific ROS metabolism in *Euglena* cells. Silencing experiments suggested that cytosolic Prxs and NTR were critical for the normal cell growth and division rather than organelle-type enzymes in *Euglena* cells (Tamaki et al., 2014; Tamaki et al., 2015). These findings may explain the physiological importance of cytosolic redox regulation in this alga. *Euglena* GPX, which use GSH as electron donor, can reduce both H_2O_2 and alkyl hydroperoxides, and is localized in the cytosol

(Overbaugh and Fall, 1985), while the gene encoding this enzyme has not yet been identified. Previous study have been demonstrated the existence of TRYR enzyme in *Euglena* (Montrichard et al., 1999), suggested that *Euglena* is a unusual organism that possesses three distinct redox systems mediated by GSH, $T(SH)_2$, and Trx. However, little is known about physiological roles and functional relationship of these thiol-based redox pathways.

To clarify physiological significance of GSH and $T(SH)_2$-mediated metabolisms in *Euglena* cells, I herein identified cDNA sequences encoding putative GR (EgGR) and TRYR (EgTRYR) by BLAST search of our *Euglena* RNA-Seq data (Ishikawa et al., unpublished data). I then examined the effect of suppression of EgGR and EgTRYR on cell growth. I also performed combined analysis with knockdown (KD) of gene encoding putative GSH synthetase, and discussed the novel molecular mechanism underlying unusual thiol-based redox metabolisms in *Euglena* cells.

Materials and Methods

Cell culture.

Euglena gracilis, strain Z, was maintained by regular subculturing and was grown in heterotrophic Koren–Hutner (KH) medium (Koren and Hutner, 1967) under continuous illumination (50 $\mu mol \cdot m^{-2} \cdot s^{-1}$) at 26 °C for 7 days, by which time the stationary phase was reached. Cell number was counted using an electric field multi-channel cell counting system, CASY (Roche Diagnostics).

RNA interference (RNAi) experiments.

The KD of EgGR, EgTRYR, and EgGSH2 by RNAi was performed as described previously (Tamaki et al., 2015). Approximately 500-bp partial cDNA templates of EgGR, EgTRYR, and EgGSH2 with the T7 RNA polymerase promoter (underlined in the primer sequences below) were amplified using the following primer sets EgGR/RNAi-F (TAATACGACTCACTATAGGGGACCTTCATTATGCGAAGTC), EgGR/RNAi-R (TAATACGACTCACTATAGGGATTTCCGTGCAGAGATGG), EgTRYR/RNAi-F (TAATACGACTCACTATAGGGAGGGCATCAACCAATCATAC),

EgTRYR/RNAi-R (TAATACGACTCACTATAGGGTTCCGTCTTCCTGTCGTTC), EgGSH2/RNAi-F (TAATACGACTCACTATAGGGACAAGGAGGTGGTGTTGGTG), and EgGSH2/RNAi-R (TAATACGACTCACTATAGGGAAATGGCGGTCAGCATCC). Double-stranded RNA (dsRNA) was synthesized from PCR products as templates using the MEGAscript RNAi Kit (Life Technologies) according to the manufacturer's instructions. *Euglena* cells from two-day-old cultures grown in KH medium were harvested and resuspended in KH medium. Approximately 15 μg of dsRNA was introduced into the cell suspension (100 μL; approximately 1×10^6 cells) using the NEPA21 electroporator (Nepa Gene). The cell suspension was inoculated into fresh medium and cultured at 26 °C for restoration.

RT-PCR analysis.

Total RNAs were isolated from 6-day-old *Euglena* cells into which dsRNA were introduced, as previously described (Tamaki et al., 2014). First strand cDNA was synthesized using PrimeScript™ RT reagent Kit with gDNA Eraser (Takara) according to the manufacturer's instructions. Gene silencing was then confirmed by RT-PCR using RNAi primer sets as described above. EgEFα was chosen as a control using the following primers; EgEF1α-F (5'-GCCTCTTCGCCTCCCACTG-3'), and EgEF1α-R (5'-TTCATCAGGACAATCGCAGCA-3'). PCR amplification was performed with 18–30 cycles of 95 °C for 30s, 58 °C for 30s, and 72 °C for 40s. The PCR products were analyzed on 1% agarose gels. Equal loading of each amplified gene sequence was determined with the control EgEF1α PCR product.

Crude extract from Euglena cells.

Euglena cells were collected by brief centrifugation and suspended in three volumes of an ice-cold buffer (10 mM potassium phosphate buffer, pH 6.8) and disrupted by sonication. The cell lysate was centrifuged at 40,000 rpm at 4 °C for 30 min and the supernatant was used for the assay of GR activity.

Enzyme assay.

GR activity was measured as the decrease in absorbance at 340 nm (ε = 6.22

mM^{-1} cm^{-1}) due to NADPH oxidation according to Shigeoka et al. (1987b). The reaction mixture contained 1 mM EDTA, 0.2 mM NADPH, and 1 mM GSSG in 50 mM potassium phosphate buffer, pH 8.2, in a final volume of 1 mL. The reaction mixture was preincubated for 1 min and started by the addition of GSSG. NADPH consumption was monitored by the decrease in absorbance at 35 °C for 1 min.

Glutathione determination.

The extraction and determination of GSH and GSSG from *Euglena* cells were performed according to the method described by Shigeoka et al. (1987b). *Euglena* cells were collected and suspended in 1 mL of 6% (v/v) perchloric acid. The cells were disrupted by sonication. The homogenate was centrifuged at 10,000 g for 20 min at 4 °C. The supernatant was adjusted to pH 7.5 by 1.25 M potassium carbonate. The solution was centrifuged at 10,000 g for 20 min at 4 °C, and the supernatant was used for the assay of GSH and GSSG. The total GSH was determined with an enzymic recycling assay based on glutathione reductase. The reaction mixture contained 100 mM potassium phosphate buffer, pH 7.5, 5 mM EDTA, 0.2 mM NADPH, 0.6 mM 5,5'-dithiobis-(2-nitrobenzoic acid) and cell extract in a final volume of 1 ml. The reaction was started by the addition of 0.5 units GR (Oriental Yeast) and absorbance at 412 nm was monitored for 1 min. GSSG was selectively determined by assaying samples in which glutathione was masked by pretreatment with 2-vinylpyrimidine. To 200 μL of sample was added 1 μL of 2-vinylpyrimidine; after being vigorously mixed for 1 min the solution was left at room temperature for 30 min, after which time it was assayed as described above. The difference between total glutathione and GSSG contents is presented as the GSH content.

Results and Discussion

Identification and primary structures of GR and TRYR in Euglena

The putative genes encoding GR and TRYR were identified from our *Euglena* RNA-Seq data (Ishikawa et al., unpublished data) by BLAST search, designated as *EgGR* and *EgTRYR*, respectively. The cDNA sequence of *EgTRYR* contained a spliced leader (SL) sequence, a motif of *Euglena* transcripts generated by trans-splicing at

their 5’ end (Tessier et al., 1991), indicated that at least *EgTRYR* cDNA sequence was full-length cDNA. Previous study showed that TRYR enzyme purified from *Euglena* cells contained peptide 1 (KMGATIRDFYTTIGVH) and peptide 2 (KVVTDHGTGYVLGV) by peptide sequence determination (Montrichard et al., 1999). The partial amino acid sequence Lys457-His472 of EgTRYR was completely identical to peptide 1, and its Lys425-Val438 was 93% identical to peptide 2 (**Figure IV-1**), strongly suggested EgTRYR protein with TRYR activity. While EgGR had high identity with known GR from *Arabidopsis thaliana*, *Chlamydomonas reinhardtii*, *Homo sapiens*, and *Escherichia coli* (40-51%), it also had similar identity with EgTRYR (52%) and known TRYR from *Trypanosoma cruzi*, *T. brucei*, *Leishmania major*, and *Crithidia fasciculata* (46-49%). The calculated molecular masses of EgGR and EgTRYR were 52.3 and 53.4 kDa, respectively, nearly identical to native enzymes of *Euglena* GR (50 kDa) and TRYR (54 kDa) described previously (Montrichard et al., 1999).

The sequence alignment of EgGR and EgTRYR with the known GR and TRYR was shown in **Figure IV-1**. EgGR, in which SL sequence was absent, contained highly conserved N-terminal region of GR from other organisms, indicated that at least sequence information of EgGR required for its enzyme function was obtained. EgGR and EgTRYR included the conserved pyridine nucleotide-disulphide oxidoreductases class-I active site (Gly52-Pro62 in EgGR, and Gly59-Pro69 in EgTRYR). In addition, these sequences also had the FAD and NADPH binding sites (Seo et al., 2006; Castro-Pinto et al., 2008). TcTRYR and TbTRYR conserved six residues interacting with TS_2, including those involved in binding the spermidine moiety (Zhang et al., 1996; Jones et al., 2010). Five of these residues were conserved in EgTRYR, but only two in EgGR. Considering that native *Euglena* GR and TRYR enzymes specifically react with GSSG and TS_2, respectively (Montrichard et al., 1999), the difference of these residues between EgGR and EgTRYR may create their strict substrate specificities.

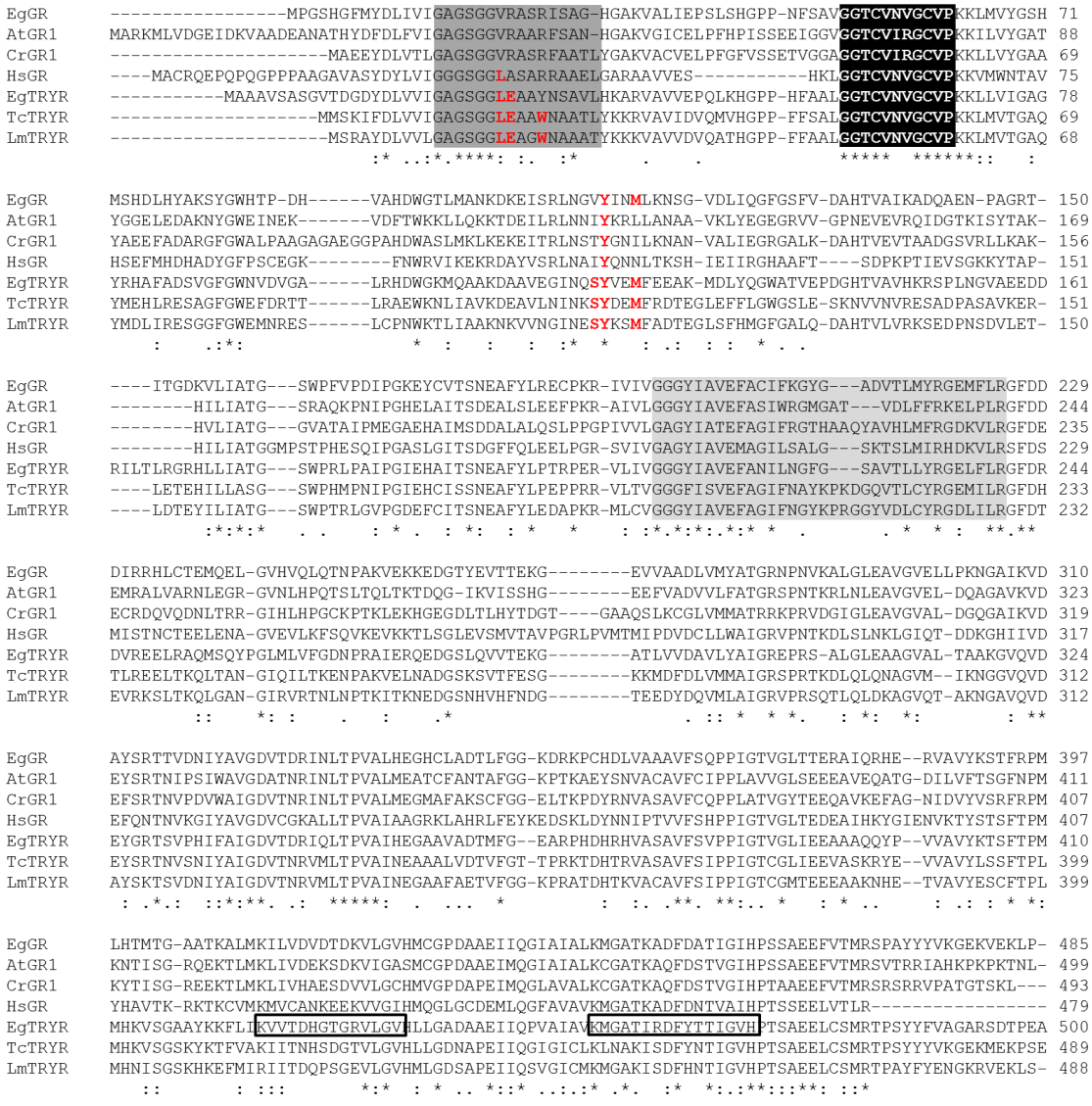

Figure IV-1. Amino acid sequence alignment of *Euglena* GR and TRYR with known GR and TRYR. Comparison of the predicted amino acid sequences of EgGR and EgTRYR with GR from *Arabidosis thaliana* (AtGR1, P48641), *Chlamydomonas reinhardtii* (CrGR1, A8HXA6), and *Homo sapiens* (HsGR, P00390), and TRYR from *Trypanosoma cruzi* (TcTRYR, P28593), *T. brucei* (TbTRYR, P39051), and *Leishmania major* (LmTRYR, Q4QJG7). Letters shown in white on a black background represent conserved pyridine nucleotide-disulphide oxidoreductases class-I active site. FAD and NADPH binding sites are highlighted in dark gray and light gray, respectively. The boxes represent the peptide sequences identified from native *Euglena* TRYR. Red letters represent conserved residues interacting with TS_2. Asterisks indicate the amino

acids conserved in all sequences, and colons and dots indicate amino acids with similar biochemical characteristics.

Previous study reported that 97% of GR activity was detected in the cytosolic fraction prepared from *Euglena* cells, indicated that *Euglena* GR was localized in the cytosol, as well as other enzymes of AsA-GSH cycle including APX, DHAR, and MDAR (Shigeoka et al., 1987b). Prediction of the subcellular localization of EgTRYR was performed using the TargetP (http://www.cbs.dtu.dk/services/TargetP/) and the TMHMM (http://www.cbs.dtu.dk/services/TMHMM/) programs. As the plastid-targeted proteins in *Euglena* had two hydrophobic regions at the N-terminal as a class I plastid-targeted motif (Durnford and Gray, 2006), TMHMM program was suitable to predict the existence of plastid-targeted signal motif in *Euglena*. Both programs indicated that EgTRYR had no characteristic signal motif (**Figure IV-2**), suggested the localization of EgTRYR in the cytosol. This prediction was well-corresponding to the fact that TRYRs from trypanosomatids were cytosolic enzymes (Smith et al., 1991; Krauth-Siegel and Comini, 2008).

A

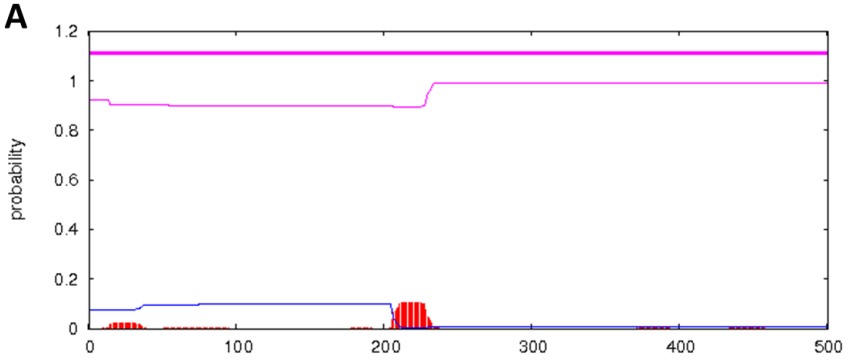

B

Name	cTP	mTP	SP	Other	Loc
EgTRYR	0.076	0.095	0.118	0.805	—

Figure IV-2. Prediction of subcellular localization of EgTRYR. (A) Prediction of transmembrane domain of using the TMHMM program. (B) Prediction of subcellular localization using the TargetP program. Values represent the possibility of the chloroplast transit peptide (cTP), mitochondrial-targeting peptide (mTP), and secretory pathway signal peptide (SP).

Effect of EgGR and EgTRYR suppression on cell growth

To evaluate the physiological significance of GR and TRYR in *Euglena* cells, I transiently suppressed *EgGR* and *EgTRYR* gene expression by introducing individual dsRNAs into *Euglena* cells using electroporation. To examine the functional relationship between GSH and $T(SH)_2$ metabolisms, double-KD *Euglena* cells, which were simultaneously suppressed *EgGR* and *EgTRYR* gene expression, were also generated. RT-PCR analysis showed that corresponding gene expression in all KD cells was specifically suppressed (**Figure IV-3A**). Total GR activities in KD-*gr* and -*gr/tryr* cells were 17 and 6% that of the control cells, respectively (**Figure IV-3B**), suggested that identified EgGR functioned as single GR enzyme in *Euglena* cells. The growth rates of KD-*gr* and -*tryr* cells were significantly lower than that of control cells under normal heterotrophic growth conditions. Interestingly, the growth rate of KD-*gr*/*tryr* was similar to that of control cells (**Figure IV-3C**). A preliminary analysis showed that

total glutathione contents of each KD cell were similar to that of control cells, while both KD-*gr* and -*gr/tryr* cells tended to accumulate GSSG (data not shown), likely suggested that EgGR was responsible for the cellular homeostasis of GSH redox ratio.

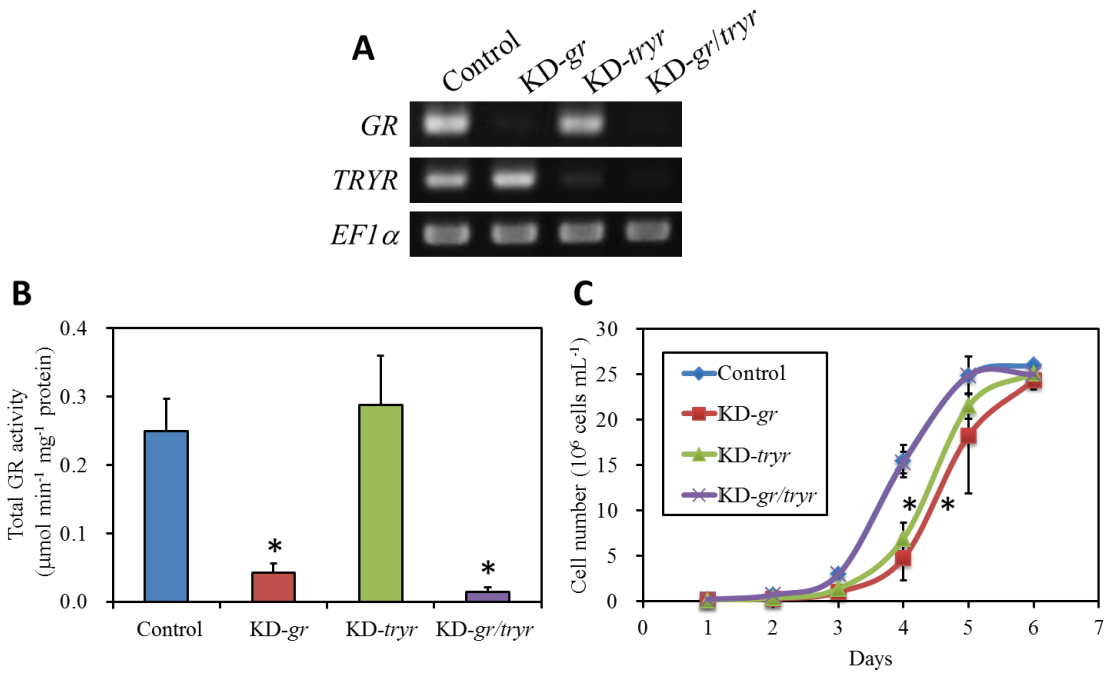

Figure IV-3. Effect of the suppression of EgGR and EgTRYR on cell growth. (A) RT-PCR analysis of *EgGR*, *EgTRYR*, and *EF1α* (for constitutive control) expression levels using total RNA from control (-dsRNA) and KD-*gr*, -*tryr*, and *gr/tryr* cells. (B) Total GR activities in crude extracts from *Euglena* cells. Values are the mean ± SD (n = 3). Asterisks indicate significantly different according to the *t*-test ($p < 0.01$). (C) Growth rates of the control and each KD cell. Cells were grown heterotrophically under continuous light (50 μmol m^{-2} s^{-1}) at 26°C for 6 days. Values are the mean ± SD (n = 3). Asterisks indicate significantly different, according to the ANOVA ($p < 0.01$).

I hypothesized that the phenotypic recovery in KD-*gr/tryr* cells was due to the facilitation of GSH biosynthetic pathway under impaired conditions of GSH and $T(SH)_2$ recycling systems. As there was no genetic information on GSH biosynthesis in *Euglena*, I obtained the putative cDNA sequence encoding glutathione synthetase (GSH2) from *Euglena* RNA-Seq data by BLAST search, designated *EgGSH2*. *EgGSH2* was defined as full-length cDNA sequence by the existence of SL sequence. EgGSH2 had high identity (34~38%) with GSH2s from other organisms including *A. thaliana*, *C. reinhardtii*, *H. sapiens*, and *S. cerevisiae*. To examine the role of GSH biosynthesis in KD-*gr/tryr* cells, KD-*gsh2* and -*gr/tryr/gsh2* cells were generated. A preliminary analysis showed that the growth rate of KD-*gsh2* was decreased as well as KD-*gr* and -*tryr* cells, while that of KD-*gr/tryr/gsh2* cells was similar to those of control and KD-*gr/tryr* cells (data not shown). Taken together, EgGR and EgTRYR enzymes were physiologically important in *Euglena* cells, whereas this organism may be capable of growing by GSH and $T(SH)_2$ metabolisms-independent manner.

In trypanosomatids, $T(SH)_2$ is central thiol that delivers electron for the cellular processes such as ROS metabolism (Castro and Tomás, 2008). Physiological significance of $T(SH)_2$ metabolism have been demonstrated by the fact that *T. brucei tryr* knockout mutant displays avirulent and increased sensitivity to H_2O_2 (Krieger et al., 2000). In case of plants, *Arabidopsis* GRs have been shown to play essential role in cellular processes such as the root growth and phytohormone signaling (Mhamdi et al., 2010; Yu et al., 2013). The growth inhibition in *Euglena* KD-*gr* and -*tryr* cells was supported by these findings, but not in KD-*gr/tryr* cells (**Figure IV-3C**). In pathogenic amoeba *Naegleria fowleri*, the co-existence of GR and TRYR also have been reported (Ondarza et al., 2006), while a relationship between GSH and $T(SH)_2$ metabolisms remains unclear so far. The growth recovery in KD-*gr/tryr* cells may have occurred due to compensation of GSH and $T(SH)_2$ pathways by Trx system. It has been demonstrated that there was functional redundancy in GSH and Trx pathways by biochemical and genetic assays in *Arabidopsis* (Reichheld et al., 2007; Marty et al., 2009). Like plants, yeast GSH pathway also acts as a functional backup system for Trx pathway (Toledano et al., 2013). Therefore, further analysis combined EgGR and EgTRYR with EgNTR will provide a fully understanding of thio-based redox metabolism in *Euglena* cells.

Abstract

Euglena gracilis contains two NADPH-dependent disulfide oxidoreductase, glutathione reductase (EgGR) and trypanothione reductase (EgTRYR). In this study, I identified the cDNA sequences encoding EgGR and EgTRYR, and characterized physiological role of them. EgTRYR contained two peptide sequences identified from native *Euglena* TRYR previously. *Euglena* GR has been shown to localize in the cytosol, EgTRYR is also predicted in the cytosol. The suppression of *EgGR* and *EgTRYR* gene expression by gene silencing resulted in significant growth inhibition, but not in simultaneous suppressed cells of both genes, in which total GR activity was nearly disappeared. These results suggested that glutathione and trypanothione-mediated redox systems were physiologically important in *Euglena* cells, while *Euglena* was capable of growing by GR and TRYR-independent manner.

REFERENCES

Apel K, Hirt H (2004) Reactive oxygen species: metabolism, oxidative stress, and signal transduction. Annual Review of Plant Biology **55**, 373-399.

Araie H, Suzuki I, Shiraiwa Y (2008) Identification and characterization of a selenoprotein, thioredoxin reductase, in a unicellular marine haptophyte alga, *Emiliania huxleyi*. The Journal of Biological Chemistry **283**, 35329-35336.

Arnér ES, Holmgren A (2000) Physiological functions of thioredoxin and thioredoxin reductase. European Journal of Biochemistry **267**, 6102-6109.

Bernier-Villamor L, Navarro E, Sevilla F, Lázaro JJ (2004) Cloning and characterization of a 2-Cys peroxiredoxin from *Pisum sativum*. The Journal of Experimental Botany **55**, 2191-2199.

Bhatt I, Tripathi BN (2011) Plant peroxiredoxins: catalytic mechanisms, functional significance and future perspectives. Biotechnology Advances **29**, 850-859.

Bowler C, Slooten L, Vandenbranden S, De Rycke R, Botterman J, Sybesma C, Van Montagu M, Inzé D (1991) Manganese superoxide dismutase can reduce cellular damage mediated by oxygen radicals in transgenic plants. The EMBO Journal **10**, 1723-1732.

Bradford MM (1976) A rapid and sensitive method for the quantitation of microgram quantities of protein utilizing the principle of protein-dye binding. Analytical Biochemistry **72**, 248–254.

Castro H, Tomás AM (2008) Peroxidases of trypanosomatids. Antioxidants & Redox Signaling **10**, 1593-1606.

Castro-Pinto DB, Genestra M, Menezes GB, Waghabi M, Gonçalves A, De Nigris Del Cistia C, Sant'Anna CM, Leon LL, Mendonça-Lima L (2008) Cloning and expression of trypanothione reductase from a New World *Leishmania* species. Archives of Microbiology **189**, 375-384.

Cejudo FJ, Ferrández J, Cano B, Puerto-Galán L, Guinea M (2012) The function of the NADPH thioredoxin reductase C-2-Cys peroxiredoxin system in plastid redox regulation and signaling. FEBS Letters **586**, 2974-2980.

Chew O, Whelan J, Millar AH (2003) Molecular definition of the ascorbate-glutathione cycle in *Arabidopsis* mitochondria reveals dual targeting of antioxidant defenses in

plants. The Journal of Biological Chemistry **278**, 46869-46877.

Comini M, Menge U, Flohé L (2003) Biosynthesis of trypanothione in *Trypanosoma brucei brucei*. Biological Chemistry **384**, 653-656.

Cramer M, Myers (1952) Growth and photosynthetic characteristics of *Euglena gracilis*. Archives of Mikrobiology **17**, 384-402.

Dayer R, Fischer BB, Eggen RI, Lemaire SD (2008) The peroxiredoxin and glutathione peroxidase families in *Chlamydomonas reinhardtii*. Genetics **179**, 41-57.

Dietz KJ (2003) Plant peroxiredoxins. Annual Review of Plant Biology **54**, 93-107.

Dietz KJ, Jacob S, Oelze M, Laxa M, Tognetti V, de Miranda SM, Baier M, Finkemeier I (2006) The function of peroxiredoxins in plant organelle redox metabolism. The Journal of Experimental Botany **57**, 1697-1709.

Dietz KJ (2011) Peroxiredoxins in plants and cyanobacteria. Antioxidants & Redox Signaling **15**, 1129-1159.

Ding Y, Liu Y, Jian JC, Wu ZH, Miao JL (2012) Molecular cloning and expression analysis of glutathione reductase gene in *Chlamydomonas* sp. ICE-L from Antarctica. Marine Genomics **5**, 59-64.

Durnford DG, Gray MW (2006) Analysis of *Euglena gracilis* plastid-targeted proteins reveals different classes of transit sequences. Eukaryotic Cell **5**, 2079-2091.

Dwyer MR, Smillie RM (1970) A light-induced β-1,3-glucan breakdown associated with the differentiation of chloroplasts in *Euglena gracilis*. Biochimica et Biophysica Acta **216**, 392-401.

Fairlamb AH, Blackburn P, Ulrich P, Chait BT, Cerami A (1985) Trypanothione: a novel bis(glutathionyl)spermidine cofactor for glutathione reductase in trypanosomatids. Science **227**, 1485-1487.

Fairlamb AH, Cerami A (1992) Metabolism and functions of trypanothione in the Kinetoplastida. Annual Review of Microbiology **46**, 695-729.

Flohé L, Budde H, Bruns K, Castro H, Clos J, Hofmann B, Kansal-Kalavar S, Krumme D, Menge U, Plank-Schumacher K, Sztajer H, Wissing J, Wylegalla C, Hecht HJ (2002) Tryparedoxin peroxidase of *Leishmania donovani*: molecular cloning, heterologous expression, specificity, and catalytic mechanism. Archives of Biochemistry and Biophysics **397**, 324-335.

Fomenko DE, Koc A, Agisheva N, Jacobsen M, Kaya A Malinouski M, Rutherford JC,

Siu KL, Jin DY, Winge DR, Gladyshev VN (2011) Thiol peroxidases mediate specific genome-wide regulation of gene expression in response to hydrogen peroxide. Proceedings of the National Academy of Sciences of the United States of America **108**, 2729-2734.

Foyer CH, Noctor G (2005) Redox homeostasis and antioxidant signaling: a metabolic interface between stress perception and physiological responses. The Plant Cell **17**, 1866-1875.

Foyer CH, Shigeoka S (2011) Understanding oxidative stress and antioxidant functions to enhance photosynthesis. Plant Physiology **155**, 93-100.

Gilberger TW, Walter RD, Müller S (1997) Identification and characterization of the functional amino acids at the active site of the large thioredoxin reductase from *Plasmodium falciparum*. The Journal of Biological Chemistry **272**, 29584-29589.

Gill SS, Anjum NA, Hasanuzzaman M, Gill R, Trivedi DK, Ahmad I, Pereira E, Tuteja N (2013) Glutathione and glutathione reductase: a boon in disguise for plant abiotic stress defense operations. Plant Physiology and Biochemistry **70**, 204-212

Holmgren A, Sengupta R (2010) The use of thiols by ribonucleotide reductase. Free Radical Biology and Medicine **49**, 1617-1628.

Inui H, Miyatake K, Nakano Y, Kitaoka S (1982) Wax ester fermentation in *Euglena gracilis*. FEBS Letters **150**, 89-93.

Iqbal A, Yabuta Y, Takeda T, Nakano Y, Shigeoka S (2006) Hydroperoxide reduction by thioredoxin-specific glutathione peroxidase isoenzymes of *Arabidopsis thaliana*. FEBS Journal **273**, 5589-5597.

Iseki M, Matsunaga S, Murakami A, Ohno K, Shiga K, Yoshida K, Sugai M, Takahashi T, Hori T, Watanabe M (2002) A blue-light-activated adenylyl cyclase mediates photoavoidance in *Euglena gracilis*. Nature **415**, 1047-1051.

Ishikawa T, Takeda T, Shigeoka S, Hirayama O, Mitsunaga T (1993) Hydrogen peroxide generation in organelles of *Euglena gracilis*. Phytochemistry **33**, 1297-1299.

Ishikawa T, Shigeoka S (2008) Recent advances in ascorbate biosynthesis and the physiological significance of ascorbate peroxidase in photosynthesizing organisms. Bioscience, Biotechnology, and Biochemistry **72**, 1143-1154.

Ishikawa T, Tajima N, Nishikawa H, Gao Y, Rapolu M, Shibata H, Sawa Y, Shigeoka S

(2010) *Euglena gracilis* ascorbate peroxidase forms an intramolecular dimeric structure: its unique molecular characterization. Biochemical Journal **426**, 125-134.

Jacquot JP, Eklund H, Rouhier N, Schürmann P (2009) Structural and evolutionary aspects of thioredoxin reductases in photosynthetic organisms. Trends in Plant Science **14**, 336-43.

Jones DC, Ariza A, Chow WH, Oza SL, Fairlamb AH (2010) Comparative structural, kinetic and inhibitor studies of *Trypanosoma brucei* trypanothione reductase with *T. cruzi*. Molecular and Biochemical Parasitology **169**, 12-19.

Kataya AR, Reumann S (2010) *Arabidopsis* glutathione reductase 1 is dually targeted to peroxisomes and the cytosol. Plant Signaling & Behavior **5**, 171-175.

Kim JA, Park S, Kim K, Rhee SG, Kang SW (2005) Activity assay of mammalian 2-cys peroxiredoxins using yeast thioredoxin reductase system. Analytical Biochemistry **338**, 216-223.

Kim JS, Bang MA, Lee S, Chae HZ, Kim K (2010) Distinct functional roles of peroxiredoxin isozymes and glutathione peroxidase from fission yeast, *Schizosaccharomyces pombe*. BMB Reports **43**, 170-175.

Kirchsteiger K, Ferrández J, Pascual MB, González M, Cejudo FJ (2012) NADPH thioredoxin reductase C is localized in plastids of photosynthetic and nonphotosynthetic tissues and is involved in lateral root formation in *Arabidopsis*. The Plant Cell **24**, 1534-1548.

König J, Baier M, Horling F, Kahmann U, Harris G, Schürmann P, Dietz KJ. (2002) The plant-specific function of 2-Cys peroxiredoxin-mediated detoxification of peroxides in the redox-hierarchy of photosynthetic electron flux. Proceedings of the National Academy of Sciences of the United States of America **99**, 5738-5743.

König J, Lotte K, Plessow R, Brockhinke A, Baier M, Dietz KJ (2003) Reaction mechanism of plant 2-Cys peroxiredoxin: Role of the C terminus and the quaternary structure. The Journal of Biological Chemistry **278**, 24409-24420.

Koren LE, Hutner SH (1967) High-yield media for photosynthesizing *Euglena gracilis*. The Journal of Protozoology **14**, 17.

Krauth-Siegel RL, Comini MA (2008) Redox control in trypanosomatids, parasitic protozoa with trypanothione-based thiol metabolism. Biochimica et Biophysica Acta **1780**, 1236-1248.

Krieger S, Schwarz W, Ariyanayagam MR, Fairlamb AH, Krauth-Siegel RL, Clayton C (2000) Trypanosomes lacking trypanothione reductase are avirulent and show increased sensitivity to oxidative stress. Molecular Microbiology **35**, 542-552.

Krnáčová K, Vesteg M, Hampl V, Vlček Č, Horváth A (2012) *Euglena gracilis* and Trypanosomatids possess common patterns in predicted mitochondrial targeting presequences. Journal of Molecular Evolution **75**, 119-129.

Laloi C, Rayapuram N, Chartier Y, Grienenberger JM, Bonnard G, Meyer Y (2001) Identification and characterization of a mitochondrial thioredoxin system in plants. Proceedings of the National Academy of Sciences of the United States of America **98**, 14144-14149.

Ledford HK, Chin BL, Niyogi KK (2007) Acclimation to singlet oxygen stress in *Chlamydomonas reinhardtii*. Eukaryotic Cell **6**, 919-930.

Machida T, Kato E, Ishibashi A, Sato J, Kawasaki S, Niimura Y, Honjoh K, Miyamoto T (2009) Expression pattern of a chloroplast NADPH-dependent thioredoxin reductase in *Chlorella vulgaris* during hardening and its interaction with 2-Cys peroxiredoxin. Bioscience, Biotechnology, and Biochemistry **73**, 695-701.

Marty L, Siala W, Schwarzländer M, Fricker MD, Wirtz M, Sweetlove LJ, Meyer Y, Meyer AJ, Reichheld JP, Hell R (2009) The NADPH-dependent thioredoxin system constitutes a functional backup for cytosolic glutathione reductase in *Arabidopsis*. Proceedings of the National Academy of Sciences of the United States of America **106**, 9109-9114.

Mhamdi A, Hager J, Chaouch S, Queval G, Han Y, Taconnat L, Saindrenan P, Gouia H, Issakidis-Bourguet E, Renou JP, Noctor G (2010) *Arabidopsis* GLUTATHIONE REDUCTASE1 plays a crucial role in leaf responses to intracellular hydrogen peroxide and in ensuring appropriate gene expression through both salicylic acid and jasmonic acid signaling pathways. Plant Physiology **153**, 1144-1160.

Miao Y, Lv D, Wang P, Wang XC, Chen J, Miao C, Song CP (2006) An *Arabidopsis* glutathione peroxidase functions as both a redox transducer and a scavenger in abscisic acid and drought stress responses. The Plant Cell **18**, 2749-2766.

Michalska J, Zauber H, Buchanan BB, Cejudo FJ, Geigenberger P (2009) NTRC links built-in thioredoxin to light and sucrose in regulating starch synthesis in chloroplasts and amyloplasts. Proceedings of the National Academy of Sciences of the United

States of America **106**, 9908-9913.

Mittler R, Vanderauwera S, Gollery M, Van Breusegem F (2004) Reactive oxygen gene network of plants. Trends in Plant Science **9**, 490-498.

Montrichard F, Le Guen F, Laval-Martin DL, Davioud-Charvet E (1999) Evidence for the co-existence of glutathione reductase and trypanothione reductase in the non-trypanosomatid Euglenozoa: *Euglena gracilis* Z. FEBS Letters **442**, 29-33.

Müller S, Gilberger TW, Färber PM, Becker K, Schirmer RH, Walter RD (1996) Recombinant putative glutathione reductase of *Plasmodium falciparum* exhibits thioredoxin reductase activity. Molecular and Biochemical Parasitology **80**, 215-219.

Müller S, Liebau E, Walter RD, Krauth-Siegel RL (2003) Thiol-based redox metabolism of protozoan parasites. Trends in Parasitology **19**, 320-328.

Navrot N, Collin V, Gualberto J, Gelhaye E, Hirasawa M, Rey P, Knaff DB, Issakidis E, Jacquot JP, Rouhier N (2006) Plant glutathione peroxidases are functional peroxiredoxins distributed in several subcellular compartments and regulated during biotic and abiotic stresses. Plant Physiology **142**, 1364-1379.

Nakano Y, Urade Y, Urade R, Kitaoka S (1987) Isolation, purification, and characterization of the pellicle of *Euglena gracilis* z. The Journal of Biochemistry **102**, 1053-1063.

Noctor G, Foyer CH (1998) Ascorbate and glutathione: keeping active oxygen under control. Annual Review of Plant Physiology and Plant Molecular Biology **49**, 249-279.

Noctor G, Gomez L, Vanacker H, Foyer CH (2002) Interactions between biosynthesis, compartmentation and transport in the control of glutathione homeostasis and signaling. The Journal of Experimental Botany **53**, 1283-1304.

Ondarza RN, Iturbe A, Hurtado G, Tamayo E, Ondarza M, Hernandez E (1999) *Entamoeba histolytica*: a eukaryote with trypanothione metabolism instead of glutathione metabolism. Biotechnology and Applied Biochemistry **30**, 47-52.

Ondarza RN, Hurtado G, Tamayo E, Iturbe A, Hernández E. (2006) *Naegleria fowleri*: a free-living highly pathogenic amoeba contains trypanothione/trypanothione reductase and glutathione/glutathione reductase systems. Experimental Parasitology **114**, 141-146.

Overbaugh JM, Fall R (1985) Characterization of a selenium-independent glutathione peroxidase from *Euglena gracilis*. Plant Physiology **77**, 437-442.

Oza SL, Shaw MP, Wyllie S, Fairlamb AH (2005) Trypanothione biosynthesis in *Leishmania major*. Molecular and Biochemical Parasitology **139**, 107-116.

Pascual MB, Mata-Cabana A, Florencio FJ, Lindahl M, Cejudo FJ (2011) A comparative analysis of the NADPH thioredoxin reductase C-2-Cys peroxiredoxin system from plants and cyanobacteria. Plant Physiology **155**, 1806-1816.

Peltier JB, Cai Y, Sun Q, Zabrouskov V, Giacomelli L, Rudella A, Ytterberg AJ, Rutschow H, van Wijk KJ (2006) The oligomeric stromal proteome of *Arabidopsis thaliana* chloroplasts. Molecular & Cellular Proteomics **5**, 114-133.

Piñeyro MD, Parodi-Talice A, Arcari T, Robello C (2008) Peroxiredoxins from *Trypanosoma cruzi*: virulence factors and drug targets for treatment of Chagas disease? Gene **408**, 45-50.

Poole LB, Karplus PA, Claiborne A (2004) Protein sulfenic acids in redox signaling. Annual Review of Pharmacology and Toxicology **44**, 325-347.

Pulido P, Spínola MC, Kirchsteiger K, Guinea M, Pascual MB, Sahrawy M, Sandalio LM, Dietz KJ, González M, Cejudo FJ (2010) Functional analysis of the pathways for 2-Cys peroxiredoxin reduction in *Arabidopsis thaliana* chloroplasts. The Journal of Experimental Botany **61**, 4043-4054.

Rapolu M, Ishikawa T, Sawa Y, Shigeoka S, Shibata H (2003) Post-transcriptional regulation of ascorbate peroxidase during light adaptation of *Euglena gracilis*. Plant Science **165**, 233-238.

Reichheld JP, Meyer E, Khafif M, Bonnard G, Meyer Y (2005) AtNTRB is the major mitochondrial thioredoxin reductase in *Arabidopsis thaliana*. FEBS Letters **579**, 337-342.

Reichheld JP, Khafif M, Riondet C, Droux M, Bonnard G, Meyer Y (2007) Inactivation of thioredoxin reductases reveals a complex interplay between thioredoxin and glutathione pathways in *Arabidopsis* development. The Plant Cell **19**, 1851-1865.

Richter AS, Peter E, Rothbart M, Schlicke H, Toivola J, Rintamäki E, Grimm B (2013) Posttranslational influence of NADPH-dependent thioredoxin reductase C on enzymes in tetrapyrrole synthesis. Plant Physiology **162**, 63-73.

Romero-Puertas MC, Campostrini N, Mattè A, Righetti PG, Perazzolli M, Zolla L, Roepstorff P, Delledonne M (2008) Proteomic analysis of S-nitrosylated proteins in *Arabidopsis thaliana* undergoing hypersensitive response. Proteomics **8**, 1459-1469.

Rouhier N, Jacquot JP (2002) Plant peroxiredoxins: alternative hydroperoxide scavenging enzymes. Photosynthesis Research **74**, 259-68.

Rouhier N, Jacquot JP (2005) The plant multigenic family of thiol peroxidases. Free Radical Biology and Medicine **38**, 1413-1421.

Schürmann P, Jacquot JP (2000) Plant thioredoxin systems revisited. Annual Review of Plant Physiology and Plant Molecular Biology **51**, 371-400.

Schürmann P, Buchanan BB (2008) The ferredoxin/thioredoxin system of oxygenic photosynthesis. Antioxidants & Redox Signaling **10**, 1235-1274.

Seo JS, Lee KW, Rhee JS, Hwang DS, Lee YM, Park HG, Ahn IY, Lee JS (2006) Environmental stressors (salinity, heavy metals, H_2O_2) modulate expression of glutathione reductase (GR) gene from the intertidal copepod *Tigriopus japonicus*. Aquatic Toxicology **80**, 281-289.

Serrato AJ, Pérez-Ruiz JM, Cejudo FJ (2002) Cloning of thioredoxin h reductase and characterization of the thioredoxin reductase-thioredoxin h system from wheat. Biochemical Journal **367**, 491-497.

Serrato AJ, Pérez-Ruiz JM, Spínola MC, Cejudo FJ (2004) A novel NADPH thioredoxin reductase, localized in the chloroplast, which deficiency causes hypersensitivity to abiotic stress in *Arabidopsis thaliana*. The Journal of Biological Chemistry **279**, 43821-43827.

Sevilla F, Camejo D, Ortiz-Espín A, Calderón A, Lázaro JJ, Jiménez A (2015) The thioredoxin/peroxiredoxin/sulfiredoxin system: current overview on its redox function in plants and regulation by reactive oxygen and nitrogen species. The Journal of Experimental Botany **66**, 2945-2955.

Shigeoka S, Nakano Y, Kitaoka S (1980) Metabolism of hydrogen peroxide in *Euglena gracilis* Z by L-ascorbic acid peroxidase. Biochemical Journal **186**, 377-380.

Shigeoka S, Yasumoto R, Onishi T, Nakano Y, Kitaoka S (1987a) Properties of monodehydroascorbate reductase and dehydroascorbate reductase and their participation in the regeneration of ascorbate in *Euglena gracilis*. Journal of General Microbiology **133**, 227-232.

Shigeoka S, Onishi T, Nakano Y, Kitaoka S (1987b) Characterization and physiological function of glutathione reductase in *Euglena gracilis* z. Biochemical Journal **242**, 511-515.

Shigeoka S, Ishikawa T, Tamoi M, Miyagawa Y, Takeda T, Yabuta Y, Yoshimura K (2002) Regulation and function of ascorbate peroxidase isoenzymes. The Journal of Experimental Botany **53**, 1305-1319.

Shigeoka S, Maruta T (2014) Cellular redox regulation, signaling, and stress response in plants. Bioscience, Biotechnology, and Biochemistry **78**, 1457-1470.

Sláviková S, Vacula R, Fang Z, Ehara T, Osafune T, Schwartzbach SD (2005) Homologous and heterologous reconstitution of Golgi to chloroplast transport and protein import into the complex chloroplasts of *Euglena*. Journal of Cell Science **118**, 1651–1661.

Smith K, Opperdoes FR, Fairlamb AH (1991) Subcellular distribution of trypanothione reductase in bloodstream and procyclic forms of *Trypanosoma brucei*. Molecular and Biochemical Parasitology **48**, 109-112.

Snider GW, Dustin CM, Ruggles EL, Hondal RJ (2014) A mechanistic investigation of the C-terminal redox motif of thioredoxin reductase from *Plasmodium falciparum*. Biochemistry **53**, 601-609.

Sugiyama A, Hata S, Suzuki K, Yoshida E, Nakano R, Mitra S, Arashida R, Asayama Y, Yabuta Y, Takeuchi T (2010) Oral administration of paramylon, a β-1,3-D-glucan isolated from *Euglena gracilis* Z inhibits development of atopic dermatitis-like skin lesions in NC/Nga mice. The Journal of Veterinary Medical Science **72**, 755-763.

Takeda T, Yokota A, Shigeoka S (1995) Resistance of photosynthesis to hydrogen peroxide in algae. Plant and Cell Physiology **36**, 1089-1095.

Tessier LH, Keller M, Chan RL, Fournier R, Weil JH, Imbault P (1991) Short leader sequences may be transferred from small RNAs to pre-mature mRNAs by trans-splicing in *Euglena*. The EMBO Journal **10**, 2621-2625.

Toledano MB, Delaunay-Moisan A, Outten CE, Igbaria A (2013) Functions and cellular compartmentation of the thioredoxin and glutathione pathways in yeast. Antioxidants & Redox Signaling **18**, 1699-1711.

Tzafrir I, Pena-Muralla R, Dickerman A, Berg M, Rogers R, Hutchens S, Sweeney TC, McElver J, Aux G, Patton D, Meinke D (2004) Identification of genes required for

embryo development in *Arabidopsis*. Plant Physiology **135**, 1206-1220.

Vieira Dos Santos C, Rey P (2006) Plant thioredoxins are key actors in the oxidative stress response. Trends in Plant Science **11**, 329-334.

Vivancos AP, Castillo EA, Biteau B, Nicot C, Ayté J, Toledano MB, Hidalgo E (2005) A cysteine-sulfinic acid in peroxiredoxin regulates H_2O_2-sensing by the antioxidant Pap1 pathway. Proceedings of the National Academy of Sciences of the United States of America **102**, 8875-8880.

Wilkinson SR, Obado SO, Mauricio IL, Kelly JM (2002) *Trypanosoma cruzi* expresses a plant-like ascorbate-dependent hemoperoxidase localized to the endoplasmic reticulum. Proceedings of the National Academy of Sciences of the United States of America **99**, 13453-13458.

Wilkinson SR, Horn D, Prathalingam SR, Kelly JM (2003) RNA interference identifies two hydroperoxide metabolizing enzymes that are essential to the bloodstream form of the african trypanosome. The Journal of Biological Chemistry **278**, 31640-31646.

Wood ZA, Schröder E, Robin Harris J, Poole LB (2003) Structure, mechanism and regulation of peroxiredoxins. Trends in Biochemical Sciences **28**, 32-40.

Wulff RP, Lundqvist J, Rutsdottir G, Hansson A, Stenbaek A, Elmlund D, Elmlund H, Jensen PE, Hansson M (2011) The activity of barley NADPH-dependent thioredoxin reductase C is independent of the oligomeric state of the protein: tetrameric structure determined by cryo-electron microscopy. Biochemistry **50**, 3713-3723.

Yabuta Y, Motoki T, Yoshimura K, Takeda T, Ishikawa T, Shigeoka S (2002) Thylakoid membrane-bound ascorbate peroxidase is a limiting factor of antioxidative systems under photo-oxidative stress. The Plant Journal **32**, 915-925.

Yu X, Pasternak T, Eiblmeier M, Ditengou F, Kochersperger P, Sun J, Wang H, Rennenberg H, Teale W, Paponov I, Zhou W, Li C, Li X, Palme K (2013) Plastid-localized glutathione reductase2-regulated glutathione redox status is essential for *Arabidopsis* root apical meristem maintenance. The Plant Cell **25**, 4451-4468.

Zhang Y, Bond CS, Bailey S, Cunningham ML, Fairlamb AH, Hunter WN (1996) The crystal structure of trypanothione reductase from the human pathogen *Trypanosoma cruzi* at 2.3 Å resolution. Protein Science **5**, 52-61.

PUBLICATIONS

1) Shun Tamaki, Takanori Maruta, Yoshihiro Sawa, Shigeru Shigeoka and Tahahiro Ishikawa (2014) Identification and functional analysis of peroxiredoxin isoforms in *Euglena gracilis*. Bioscience, Biotechnology, and Biochemistry 78: 593-601 (**CHAPTER II**)

2) Shun Tamaki, Takanori Maruta, Yoshihiro Sawa, Shigeru Shigeoka and Tahahiro Ishikawa (2015) Biochemical and physiological analyses of NADPH-dependent thioredoxin reductase isozymes in *Euglena gracilis*. Plant Science 236: 29-36 (**CHAPTER III**)

SUMMARY

ROS cause oxidative damage in aerobic organisms, while they also act as signaling molecules regulating cellular processes including growth and stress responses. Therefore, intracellular ROS levels must be tightly controlled. In microalga *Euglena gracilis*, cytosolic APX have been identified, while little is known about ROS metabolism in major ROS sources such as chloroplasts and mitochondria. Prx and Trx system, consisting of Trx and NTR, play crucial roles in ROS metabolism and redox regulation in almost all organisms, whereas none of genes encoding them have been analyzed yet in *Euglena*. Thus, to clarify Prx and Trx-mediated ROS metabolism and redox regulation in *Euglena*, I identified genes encoding Prx and NTR, and characterized them.

I obtained the cDNA sequences of four Prx (*EgPrx1~4*) and three NTR (*EgNTR1*, *-2*, and *-C*) gene by homology search in *Euglena* RNA-Seq data. EgPrx1, -4, and -NTR2 were predicted to be localized in the cytosol, EgPrx2 and EgNTRC in chloroplasts, and EgPrx3 and EgNTR1 in mitochondria. All recombinant EgPrxs could reduce H_2O_2 and alkyl hydroperoxides by Trx system-dependent manner. The catalytic efficiencies of these enzymes were similar to those of plant thiol-peroxidases. Also, all recombinant EgNTRs showed NADPH-dependent disulfide reduction activities, and the catalytic efficiency of EgNTR2 for NADPH was 30-46-fold higher than those of EgNTR1 and EgNTRC. Silencing experiments showed that the growth rates of KD-*prx1/4* and *-ntr2* cells were markedly reduced under normal growth conditions. In addition, cell hypertrophy in KD-*ntr2* cells was observed. These results suggested that Prxs and Trx systems contributed to cellular compartment-specific ROS metabolism, and cytosolic Prxs and NTR were physiologically important in cell growth and division.

Previous study have been suggested that *Euglena* has metabolic pathways of GSH and $T(SH)_2$, which is thiol compound existed in tyrpanosomatids. To clarify physiological role of GSH and $T(SH)_2$ metabolisms in *Euglena*, I identified genes encoding GR and TRYR, and examined the physiological role of GR and TRYR in *Euglena* cells. I obtained the cDNA sequences of *GR* (*EgGR*) and *TRYR* (*EgTRYR*) genes based on *Euglena* RNA-Seq data. Silencing experiments showed that the growth

rates of KD-*gr* and -*tryr* cells were significantly reduced, while this phenotypic change was recovered by simultaneous suppression of *EgGR* and *EgTRYR* gene expression. These results suggested that GSH and $T(SH)_2$ were physiologically important as redox buffer in *Euglena* cells, whereas *Euglena* was capable of growing by GR and TRYR-independent manner.

摘要

ROS は、過剰に蓄積すると細胞毒となるが、一方で、ROS は生育やストレス応答などを制御するシグナル伝達分子としても機能することが知られている。そのため、細胞内 ROS レベルは厳密に制御されなければならない。ユーグレナにおいて、細胞質にのみ局在する APX が同定されたが、主要な ROS 発生源である葉緑体やミトコンドリアといった細胞内コンパートメントにおける ROS 代謝は不明であった。ほぼすべての生物種において、Prx や、Trx および NTR から成る Trx システムが ROS 代謝や細胞内レドックス制御に重要な役割を果たすことが明らかにされたが、ユーグレナにおいてこれら酵素遺伝子は未同定である。そこで本研究では、Prx および Trx システムを介した ROS 代謝およびレドックス制御機構の解明を目的として、ユーグレナ Prx および NTR の同定および機能解析を行った。

ユーグレナ RNA-Seq データの相同性検索により、4 つの Prx（*EgPrx1~4*）および 3 つの NTR（*EgNTR1, -2, -C*）の cDNA 配列を取得した。EgPrx1、-4、-NTR2 は細胞質、EgPrx2、-NTRC は葉緑体、EgPrx3、-NTR1 はミトコンドリアへの局在が予測された。すべての組換え体 EgPrx が Trx システム依存的に、H_2O_2 およびアルキルヒドロペルオキシドに対する還元活性を示し、それらのカイネティクスパラメーターは植物 Prx と同程度であった。また、すべての組換え体 EgNTR がジスルフィド還元活性を示し、組換え体 EgNTR2 の触媒効率（k_{cat}/K_m）は組換え体 EgNTR1 および EgNTRC の約 30~46 倍高かった。各遺伝子ノックダウン細胞を作製したところ、KD-*prx1/4* および-*ntr2* 細胞は顕著な生育速度の低下を示し、さらに、KD-*ntr2* 細胞の肥大化が観察された。これらの結果から、ユーグレナ細胞において、Prx および Trx システムが細胞内コンパートメント特異的な ROS 代謝に寄与し、細胞質型 Prx および NTR は細胞生育および分裂に重要な役割を果たすことが示唆された。

過去の研究から、ユーグレナは、グルタチオンおよびトリパノソーマ類に特異的なトリパノチオン代謝系を持つことが示唆された。そこで本研究では、ユーグレナにおけるグルタチオンおよびトリパノチオン代謝系の生理的役割の解明を目的として、ユーグレナ GR および TRYR の同定および機能解析を行った。ユーグレナ RNA-Seq データに基づき、GR および TRYR をコードする cDNA 配列（*EgGR, -TRYR*）を取得した。KD-*gr* および-*tryr* 細胞の生育速度は有意に低

下したが、KD-*gr*/*tryr* 細胞の生育速度はコントロール細胞と同程度であった。これらの結果から、ユーグレナ細胞において、GR および TRYR が生理的に重要であるにも関わらず、それら酵素に非依存的な生育が可能であることが示唆された。